© 2014. Published by The Company of Biologists Ltd | Disease Models & Mechanisms (2014) 7, 445-458 doi:10.1242/dmm.014134

RESEARCH ARTICLE

The central molecular clock is robust in the face of behavioural arrhythmia in a *Drosophila* model of Alzheimer's disease

Ko-Fan Chen[1,*], Bernard Possidente[2], David A. Lomas[3] and Damian C. Crowther[1,4,*]

ABSTRACT

Circadian behavioural deficits, including sleep irregularity and restlessness in the evening, are a distressing early feature of Alzheimer's disease (AD). We have investigated these phenomena by studying the circadian behaviour of transgenic *Drosophila* expressing the amyloid beta peptide (Aβ). We find that Aβ expression results in an age-related loss of circadian behavioural rhythms despite ongoing normal molecular oscillations in the central clock neurons. Even in the absence of any behavioural correlate, the synchronised activity of the central clock remains protective, prolonging lifespan, in Aβ flies just as it does in control flies. Confocal microscopy and bioluminescence measurements point to processes downstream of the molecular clock as the main site of Aβ toxicity. In addition, there seems to be significant non-cell-autonomous Aβ toxicity resulting in morphological and probably functional signalling deficits in central clock neurons.

KEY WORDS: Alzheimer's disease, Circadian dysfunction, Non-cell-autonomous Aβ toxicity, *Drosophila* model, Biological clock

INTRODUCTION

Alzheimer's disease (AD) is the most common cause of dementia in adults and is characterised at the microscopic level by extracellular amyloid plaques and intraneuronal tau tangles. Amyloid plaques are composed of fibrillar aggregates of a spectrum of amyloid beta (Aβ) peptides derived from the proteolytic cleavage of amyloid precursor protein (APP) (LaFerla et al., 2007). The significance of Aβ is underpinned by the numerous disease-linked mutations that dysregulate APP processing: mutations that result in a spectrum of Aβ peptides with a higher aggregation propensity have been linked to familial AD (Philipson et al., 2010), whereas sequence variation in APP that reduces Aβ production is protective (Jonsson et al., 2012). There is much evidence from cell-culture and animal-model systems (Iijima-Ando and Iijima, 2010; Philipson et al., 2010) that the conformers of Aβ that possess neurotoxic activity are likely to be soluble oligomeric species rather than the more easily detected amyloid plaques (Lesné et al., 2006; Shankar et al., 2008; Ono et al., 2009; Tomic et al., 2009; Brorsson et al., 2010; Jo et al., 2011; Tang et al., 2012; Speretta et al., 2012).

[1]Department of Genetics, Downing Site, Cambridge, CB2 3EH, UK. [2]Biology Department and Neuroscience Program, Skidmore College, Saratoga Springs, NY 12866, USA. [3]Department of Medicine, University College London, London, W1T 7NF, UK. [4]Cambridge Institute for Medical Research, Wellcome/MRC Building, Hills Road, Cambridge, CB2 0XY, UK.

*Authors for correspondence (kc436@cam.ac.uk; dcc26@cam.ac.uk)

Received 4 September 2013; Accepted 6 February 2014

Alongside the well-recognised memory and cognitive deficits that typify AD, a substantial proportion of individuals with AD also experience circadian abnormalities, including increased daytime napping, night-time restlessness and fragmented sleep. Taken together, these clinical features constitute a dampening of the variation in day-night activity (Volicer et al., 2001; Coogan et al., 2013); furthermore, two-thirds of individuals with AD that are living at home exhibit some degree of 'sundowning', in which restlessness and agitation increase late in the afternoon and early evening (Prinz et al., 1982; Volicer et al., 2001). It is readily apparent that such behavioural problems are a substantial burden for both AD individuals and their caregivers.

Circadian timekeeping in animals is a cell-autonomous mechanism based on the intrinsic 24-hour-period oscillation of 'clock gene' products (such as PER1, PER2, CRY1, CRY2, CLOCK and BMAL1 in humans) mediated by interlocked transcriptional-translational feedback and feedforward loops (TTFLs). Such cellular circadian oscillators are present throughout the body, but those in the suprachiasmatic nucleus (SCN; ~20,000 'clock neurons') of the hypothalamus are considered to be the master pacemaker in humans (Mohawk et al., 2012). The SCN neurons are divided into a dorsal shell [arginine vasopressin (AVP)-positive] and ventral core [vasoactive intestinal polypeptide (VIP)-positive areas]. Circadian oscillators in the SCN are entrained by light to keep them in synchrony with the external light-dark cycle. The SCN then converts the entrained circadian signal into coordinated physiological and behavioural outputs via multiple humoural and neuronal pathways (Mohawk et al., 2012). Importantly, circadian oscillations are self-sustaining at both molecular and behavioural levels. Therefore 'free-running' rhythms continue even in the absence of external cues [e.g. the constant darkness (DD)].

The behavioural abnormalities linked to AD in the clinic have been substantiated by histological changes in the SCN in postmortem brains, in particular the cell loss observed by Swaab and colleagues (Swaab et al., 1985; Swaab et al., 1988). Despite the cell loss seen in the SCN in AD brains, amyloid plaques here are sparse (Coogan et al., 2013), possibly indicating that Aβ toxicity is largely non-cell-autonomous, being derived from neighbouring cells. Concordant with this, Tate and colleagues reported reduced amplitude of behavioural rhythms in rats carrying SCN grafts of PC12 cells expressing a disease-linked variant of APP as compared with animals grafted with control PC12 cells (Tate et al., 1992). However, subsequent murine studies of AD-linked circadian locomotor abnormalities, using established model systems, has yielded a complex and sometimes contradictory picture. In particular, mice expressing mutant APP in light-dark (LD) conditions exhibit normal circadian locomotor activity (Wisor et al., 2005; Ambrée et al., 2006; Gorman and Yellon, 2010). By contrast, increased locomotor activity during resting light hours was detected in transgenic animals expressing additional mutated human γ-secretase (APP×PS1) (Duncan et al., 2012) or the combination of

Disease Models & Mechanisms (2014) doi:10.1242/dmm.014134

TRANSLATIONAL IMPACT

Clinical issue

Alzheimer's disease (AD) is the commonest cause of dementia in adults. At the microscopic level, AD is characterised by two main pathologies: firstly, extracellular amyloid plaques, which are composed of amyloid beta peptide (Aβ), derived from the proteolytic cleavage of amyloid precursor protein, and secondly, intraneuronal tau tangles. At the clinical level, alongside memory deficits, abnormalities in the sleep-wake cycle are an early feature of AD. Circadian rhythmicity in humans is controlled by a molecular clock in the central clock neurons in the suprachiasmatic nucleus (SCN) of the hypothalamus. Postmortem studies suggest that the loss of cells in the SCN contributes to circadian abnormalities in AD. However, it is not known whether the clock itself is degraded or whether communication of the rhythm to the periphery is lost in disease. A better understanding of the pathological mechanisms underlying circadian abnormalities in AD would facilitate the design of effective interventions that could improve well-being and clinical outcomes in individuals with AD, and their carers.

Results

Drosophila that express toxic isoforms of Aβ in the nervous system have previously been established as a model of AD. Here, the authors show that the pan-neuronal expression of Aβ in the brains of flies results in progressive loss of circadian behavioural rhythmicity, despite ongoing normal oscillations of the central molecular clock. Circadian deficits were most marked when Aβ was expressed in neighbouring neurons and glia rather than in the clock neurons themselves, and one target for this non-cell-autonomous Aβ toxicity seems to be the paracrine communication of the clock neurons. Finally, the authors demonstrate that entrainment of the central molecular clock by exposure to regular light-dark cycles, even in the face of behavioural arrhythmia, prolongs the flies' lifespan.

Implications and future directions

This work shows clearly that, in a fly model of AD, the central molecular clock is robust in the face of behavioural arrhythmicity and that, despite having no observable influence on behaviour, an entrained clock is able to prolong life. These findings support the use of light therapy to entrain the clocks of individuals with, or at risk of, AD even if such an intervention produces no obvious behavioural response. Moreover, the discovery of a robust invertebrate model of non-cell-autonomous Aβ toxicity provides a platform for looking for ways to modulate this toxicity. The achievement of such a goal could have wide-ranging consequences for our understanding of AD that extend beyond circadian biology.

mutant PS1 and tau (APP×PS1×tau) (Sterniczuk et al., 2010). Furthermore, only minor deficits in free-running behaviour (DD) are detected in these AD model systems (Wisor et al., 2005; Gorman and Yellon, 2010; Sterniczuk et al., 2010). For these reasons, the role of toxic Aβ species in circadian deficits in AD remains elusive.

As a complement to murine models of AD, we have generated a *Drosophila* system to study Aβ toxicity. Instead of replicating the proteolytic processing of APP, we and others have fused the Aβ peptide with a secretion signal peptide and driven its expression in the nervous system (Finelli et al., 2004; Iijima et al., 2004; Crowther et al., 2005). Various Aβ species were expressed pan-neuronally in *Drosophila* using the *Gal4-UAS* expression system (Brand and Perrimon, 1993), and Aβ toxicity was detected using a range of biochemical, neuron-histological and behavioural assays (e.g. Jahn et al., 2011; Speretta et al., 2012; Huang et al., 2013). In this study we have combined the tools available to neurodegeneration modelling in the fly with the well-developed systems that are also available for studying circadian rhythms. The use of the fly as a model organism is justified by the many orthologies between *Drosophila* and human, in particular by the conserved circadian TTFLs, involving the clock genes *period*, *timeless*, *clock* and *cycle* (Allada and Chung, 2010). Circadian locomotor activity in *Drosophila* is controlled by ~150 clock-gene-expressing neurons (clock neurons) in the brain. As with the SCN in humans, *Drosophila* clock neurons can be divided into several groups (termed sLNvs, lLNvs, LNds, DN1s, DN2s, DN3s and LPNs in the fly) according to their ventral-dorsal anatomy and neuropeptide identity. Similar to the role of the neuropeptide VIP in synchronising among clock neurons in the SCN (Hastings and Herzog, 2004; Aton et al., 2005; Maywood et al., 2006), the neuropeptide PDF (pigment disperse factor), released from about 16 ventral neurons (sLNvs and lLNvs) in *Drosophila*, maintains robust circadian behaviour by paracrinely synchronising the molecular oscillation of clock neurons (e.g. Renn et al., 1999; Peng et al., 2003; Cusumano et al., 2009). In addition, the majority of the axons from these clock neurons project to the dorsal protocerebrum (dorsal commissure) (Helfrich-Förster et al., 2007), where they communicate with each other and to their downstream targets. Normal free-running circadian behaviour in *Drosophila* also requires correct signalling at these synapses (Kaneko et al., 2000; Blanchardon et al., 2001; Nitabach et al., 2002). Rezával et al. (Rezával et al., 2008) previously demonstrated that overexpression of wild-type human APP in PDF-positive ventral clock neurons (*pdf>hAPP*) resulted in age-dependent loss of circadian rhythm. Although *Drosophila* does have the γ-secretase required to process APP, it has little β-secretase-like (dBACE) activity and so the generation of Aβ peptides is inefficient (Fossgreen et al., 1998; Carmine-Simmen et al., 2009). Therefore, the circadian abnormality in *pdf>hAPP* flies (Rezával et al., 2008) is probably unrelated to toxic Aβ peptides. In this study, however, we have employed well-established tools for characterising the *Drosophila* clock system to investigate the mechanism of Aβ-mediated disruption of circadian rhythms.

RESULTS

Ubiquitous neuronal Aβ expression causes circadian behavioural deficits

To determine whether our Aβ-expressing flies (Crowther et al., 2005; Jahn et al., 2011) exhibit disturbed intrinsic circadian rhythms, we monitored their circadian locomotor activities in constant darkness (DD). By calculating autocorrelation coefficients we quantified the robustness of their circadian periodicity [arrhythmia is defined as rhythmic statistic (RS) ≤1.5] (Levine et al., 2002). The *Gal4-UAS* system was used to drive expression from a single transgene of each of $A\beta_{40}$, $A\beta_{42}$ and the arctic (E22G) variant of the $A\beta_{42}$ peptide in the *Drosophila* nervous system (*elav>Aβ40*, *elav>Aβ42* and *elav>Aβ42arc*; Fig. 1). While still young [2-12 days after eclosion (dae) and 12-22 dae], the $A\beta_{40}$ and $A\beta_{42}$ flies exhibited robust circadian rhythmicity in DD that was essentially identical to that observed in control flies (*elav>51D*). Although a subpopulation of $A\beta_{40}$- and $A\beta_{42}$-expressing flies developed arrhythmic behaviour by the age of 22-32 dae, their average RS did not differ significantly from controls (Table 1). By contrast, the overall rhythmicity of flies expressing pan-neuronal $A\beta_{42}$arc was significantly reduced compared with controls at all age groups (RS; Table 1). Furthermore, there was an age-related progression in dysrhythmia with a significant decline in the RS between the 2-12 dae and 22-32 dae groups (Table 1). At 22-32 dae, about 80% of the *elav>Aβ42arc* flies were arrhythmic, whereas the majority of the age-matched controls flies remained rhythmic (Table 1). Consistent with the age-dependent decline in circadian behaviour, the arrhythmic pattern in the averaged actogram of *elav>Aβ42arc* flies was clear by 22-32 dae (Fig. 1A). Although all flies tested exhibited age-related decline in circadian rhythmicity (Fig. 1B), those expressing $A\beta_{42}$arc were significantly worse than other genotypes. The appearance of

Disease Models & Mechanisms (2014) doi:10.1242/dmm.014134

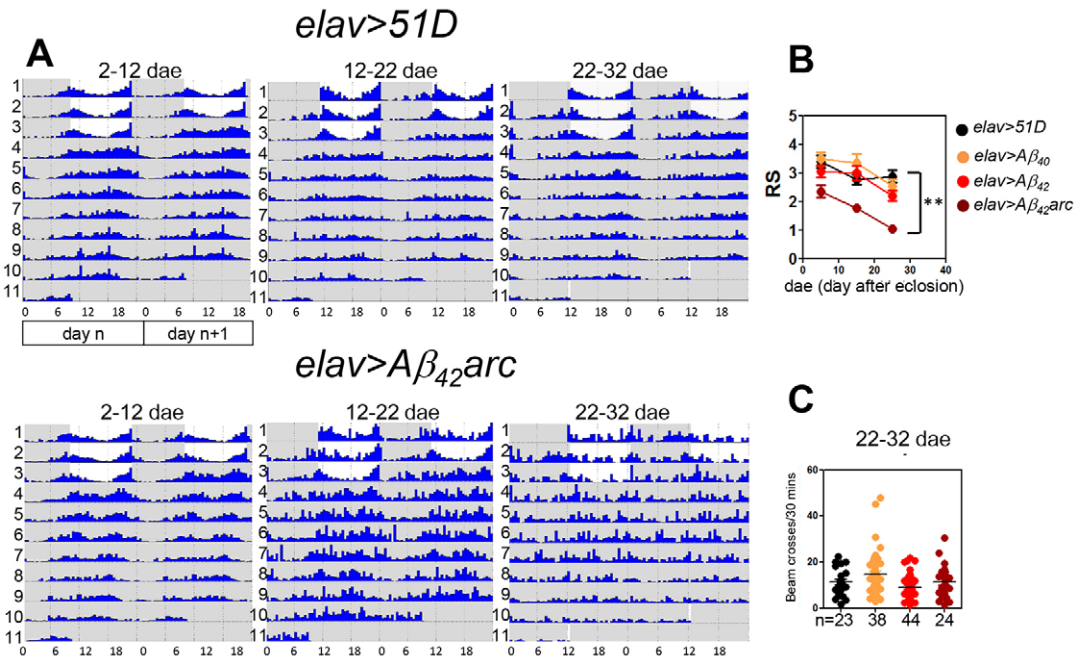

Fig. 1. Loss of circadian locomotor behaviour in Aβ$_{42}$arc-expressing flies. (A) Representative average actograms of 16 individuals at different age groups are shown for male controls (*elav>51D*, upper panels) and flies expressing Aβ$_{42}$ arctic mutant (Aβ$_{42}$arc) in all neurons (*elav>Aβ$_{42}$arc*, lower panels). Two continuous days are plotted in each row (day *n* and day *n*+1; i.e. day *n*+1 in row 1 is equivalent to day *n* in row 2), in which the *y*-axis is activity in each day and *x*-axis is the hours in each day (the white area marks the light phase; the grey shaded area marks the dark phases). The ages of the flies are indicated as day after eclosion (dae). Numbers 1-11 represent actual days under recording. (B) Reduced periodicity, determined by average rhythmic statistic (RS; mean ± s.e.m.), is found in Aβ$_{42}$arc-expressing flies compared with controls and flies expressing Aβ$_{40}$ or Aβ$_{42}$ peptide. Asterisks mark significance (P<0.01) by non-parametric one-way ANOVA between *elav>Aβ$_{42}$arc* and *elav>51D* controls. (C) No difference in average locomotor activity (i.e. mean of beam crosses) are found among indicated genotypes in the age group of 22-32 dae. Number of flies tested is indicated.

discreet Aβ deposits, akin to plaques, in Aβ$_{42}$arc fly brains (supplementary material Fig. S1A-E) correlates with the severity of behavioural disruption. However, the amount of such large Aβ aggregates in the brain does not predict behavioural arrhythmia because, for any given Aβ genotype, there is no difference in plaque density between behaviourally rhythmic and arrhythmic flies (supplementary material Fig. S1F and see Discussion).

To exclude the possibility that the age-related decline in walking velocity in Aβ-expressing flies (Jahn et al., 2011) was confounding our observations of circadian rhythmicity, we assessed the overall daily locomotor activity. When we counted the number of beam crosses in our DAM apparatus, there were no significant differences between any genotypes at least until age 22-32 dae (Fig. 1C). This indicates that the loss of circadian activity is not a function of overall decreased locomotor activity.

Once arrhythmia develops in DD it cannot be reversed by LD

Because of the characteristic dampening of circadian rhythm in individuals with AD, light treatment has been used in an attempt to enhance circadian rhythmicity (Coogan et al., 2013). To investigate the reversibility of the circadian arrhythmia in Aβ-expressing flies, we identified young flies that displayed arrhythmic behaviour when transferred from LD to DD. We then returned them to LD, with a 6-hour shift in the cycle, and looked to see whether rhythmic behaviour was restored. Flies with an intact circadian clock respond not only to the actual light changes in LD with a startle reflex but also anticipate dawn and dusk with 2-3 hours of increased locomotor activity (Stoleru et al., 2005; Lim et al., 2007). We used this circadian controlled 'anticipatory ramping' in activity as the marker of rhythmicity in these experiments. In control flies (*elav>51D*) exposed to LD, anticipatory ramping in behaviour was seen, as expected, before dawn (white circle, Fig. 2A) and dusk (black circle, Fig. 2A). In continuous darkness, control flies retained robust circadian behaviour, with one peak of activity during the 24-hour period (Fig. 2Aiii). In the following secondary LD cycles, control flies were able to re-synchronise with the new phase within 1 day (Fig. 2Ai,iv). Under the same conditions, *elav>Aβ$_{42}$arc* flies retained substantial rhythmic behaviour during the first LD cycles (Fig. 2Bi,ii) but became arrhythmic in the following constant darkness (cf. Fig. 1A; Fig. 2Bi,iii). Furthermore, *elav>Aβ$_{42}$arc* flies largely failed to re-synchronise and exhibited weak ramping activity in the secondary LD (Fig. 2Bi,iv). The Harrisingh anticipatory index was used to objectively quantify the degree of entrainment in *elav>Aβ$_{42}$arc* flies during LD (Harrisingh et al., 2007). We found that *elav>Aβ$_{42}$arc* flies have a much reduced anticipatory index as compared with the controls, and they were comparable to the non-anticipatory *period*-null mutants (*per^{01}*) during the secondary LD cycles (Fig. 2Aiv,Biv,Civ,D). Taken together, we found that none of the DD-arrhythmic *elav>Aβ$_{42}$arc* flies were able to regain vigorous rhythmicity during the subsequent LD cycles, indicating that behavioural deficits are not readily remediated by re-exposure to a rhythmic 24-hour LD cycle.

The LD environment benefits arrhythmic Aβ-expressing flies

Having established that DD-arrhythmic flies could not be substantially re-entrained by subsequent exposure to an LD environment, we were interested to know whether, despite this, a rhythmic environment could still provide benefits for an arrhythmic organism. To investigate this possibility, we took control and Aβ$_{42}$arc-expressing flies and compared their longevity in LD and

Disease Models & Mechanisms (2014) doi:10.1242/dmm.014134

Table 1. Summary of the rhythmicity and the free-running period of flies expressing various Aβ peptides in the clock system

Age group (dae)	Genotype	RS		Period (hours)		Tested number	Rhythmic number	Rhythmic percentage	Statistics		
		Median	Mean ± s.e.m.	Median	Mean ± s.e.m.				RS[a]	Period[b]	Age[c]
2-12	*elav>51D*	3.6	3.4±0.2	23.8	23.7±0.1	32	29	90.6			
	elav>Aβ40	3.6	3.5±0.3	23.8	23.7±0.1	30	27	90.0			
	elav>Aβ42	3.1	3.1±0.2	23.9	23.9±0.1	32	28	87.5			
	elav>Aβ42arc	2.1	2.4±0.2	23.8	23.8±0.1	32	24	75.0	**		
12-22	*elav>51D*	2.8	2.8±0.2	23.5	23.6±0.2	47	40	85.1			
	elav>Aβ40	2.8	3.3±0.3	23.8	23.6±0.1	23	23	100.0			
	elav>Aβ42	2.9	3.0±0.3	23.8	23.7±0.1	24	20	83.3			
	elav>Aβ42arc	1.8	1.8±0.1	23.5	23.5±0.1	48	28	58.3	***		
22-32	*elav>51D*	2.7	2.9±0.2	23.8	23.8±0.3	39	32	82.1			
	elav>Aβ40	2.4	2.6±0.2	23.5	23.6±0.1	44	33	75.0			
	elav>Aβ42	2.1	2.2±0.2	23.5	23.4±0.2	38	28	73.7			
	elav>Aβ42arc	1.3	1.1±0.1	24.7	24.7±0.4	35	8	22.9	***		**
2-12	*tim>51D*	3.8	3.8±0.3	24.3	24.1±0.1	32	29	91			
	tim>Aβ40	3.8	3.7±0.2	24.0	23.9±0.1	30	29	97			
	tim>Aβ42	3.6	3.5±0.2	24.0	23.9±0.1	30	28	93			
	tim>Aβ42arc	3.7	3.6±0.1	23.8	23.6±0.1	32	32	100			
10-22	*tim>51D*	2.8	2.8±0.1	24.2	24.1±0.1	64	54	84			
	tim>Aβ40	2.9	2.8±0.2	24.3	24.4±0.1	47	39	83			
	tim>Aβ42	3.0	3.0±0.3	24.8	24.8±0.1	16	13	81			
	tim>Aβ42arc	2.8	2.8±0.2	24.3	24.1±0.1	24	23	96			
	tim>TAβ40	3.4	3.3±0.2	24.3	24.4±0.1	32	30	94			
	tim>TAβ42	1.7	1.8±0.1	24.8	24.8±0.2	71	41	58	***	***	
18-32	*tim>51D*	2.4	2.4±0.2	24.3	24.3±0.1	59	46	78			**
	tim>Aβ40	2.5	2.7±0.1	24.0	24.1±0.1	63	53	84			
	tim>Aβ42	1.9	2.0±0.1	24.3	24.5±0.1	37	23	62			
	tim>Aβ42arc	2.2	2.3±0.2	24.3	24.3±0.1	40	32	80			
	tim>TAβ40	2.8	2.6±0.3	24.5	24.4±0.1	8	7	88			
	tim>TAβ42	1.2	1.2±0.1	25.4	25.0±0.7	38	10	26	***		
31-42	*tim>51D*	1.7	1.9±0.2	24.3	24.3±0.2	41	24	59			***
	tim>Aβ40	1.6	1.6±0.1	25.0	24.8±0.2	55	28	51			
	tim>Aβ42	1.5	1.8±0.2	25.0	24.8±0.3	42	20	48			
	tim>Aβ42arc	1.7	1.7±0.1	24.3	24.4±0.2	63	38	60			
17-27	*tim>TAβ40/8.0-luc:9*	3.1	3.4±0.4	24.5	25.0±0.3	13	12	92			
	tim>TAβ42/8.0-luc:9	1.3	1.3±0.2	24.5	25.0±0.4	11	3	27	#		
10-22	*tim,pdf-gal80>51D*	2.5	2.8±0.2	24.3	24.3±0.1	25	24	96			
	tim,pdf-gal80>TAβ40	3.1	2.7±0.2	24.3	24.4±0.1	26	20	77			
	tim,pdf-gal80>TAβ42	1.8	1.6±0.2	24.3	24.8±0.4	16	9	56	**		
24-31	*tim,pdf-gal80>TAβ40*	3.1	2.5±0.2	24.0	24.5±0.3	16	13	81			
	tim,pdf-gal80>TAβ42	1.5	1.4±0.2	24.0	24.2±0.7	15	7	47	#		
2-12	*pdf>51D*	3.7	3.4±0.2	24.3	24.2±0.1	32	30	94			
	pdf>Aβ40	3.5	3.4±0.2	24.0	24.0±0.1	32	31	97			
	pdf>Aβ42	3.6	3.6±0.2	24.3	24.2±0.1	32	32	100			
	pdf>Aβ42arc	4.4	4.2±0.2	24.0	24.1±0.1	14	14	100			
	pdf>hid	1.5	1.6±0.2	21.9	22.1±0.5	16	6	38	**	*	
18-32	*pdf>51D*	3.0	3.0±0.2	24.3	24.2±0.1	43	36	84			
	pdf>Aβ40	2.2	2.6±0.4	24.8	24.3±0.4	14	11	79			
	pdf>Aβ42	3.2	3.1±0.2	24.5	24.4±0.1	30	28	93			
	pdf>Aβ42arc	4.7	4.2±0.2	24.3	24.4±0.1	32	30	94			
	pdf>TAβ42	2.8	3.1±0.3	24.5	24.6±0.1	29	23	79			
31-42	*pdf>51D*	2.9	2.8±0.2	24.3	24.5±0.1	36	32	89			
	pdf>Aβ40	2.5	2.5±0.3	24.5	24.8±0.2	14	11	79			
	pdf>Aβ42	2.4	2.6±0.5	24.8	24.9±0.2	11	7	64			
	pdf>Aβ42arc	3.7	3.7±0.2	24.4	24.4±0.1	30	30	100			
	pdf>hid	1.7	1.5±0.2	21.3	22.2±0.7	12	7	58	***	**	

Rhythmic statistics (RS) and the period of behavioural rhythm in DD (Period) for the indicated genotypes are determined by autocorrelation (see Materials and Methods). Rhythmic number: the number of flies with RS >1.5; Tested number: total number of flies tested for each genotype/age groups; Rhythmic percentage: rhythmic number/tested number in percentage. Statistical significant difference in RS ([a]) and the period ([b]) between the indicated genotypes and the age-matched controls (*elav>51D*, *tim>51D*, *tim,pdf-gal80>51D* or *pdf>51D*) is indicated by asterisks (*P<0.05, **P<0.01, ***P<0.001) determined by non-parameteric one-way ANOVA (Dunn's post-test) or Student's *t*-test (#, compared with *tim,pdf-gal80>TAβ40* or *tim>TAβ40/8.0-luc:9*). Age-related difference in RS ([c]) in *elav>Aβ42arc* and *tim>51D* flies at the indicated age groups is determined by comparing to the 2-12 dae counterpart (one-way ANOVA, Dunn's post-test). Four *tim-gal4* driver lines [*tim(27)*, *tim(62)*, *tim(67)* and *tim(86)*] are used in this set of behaviour tests.

Disease Models & Mechanisms (2014) doi:10.1242/dmm.014134

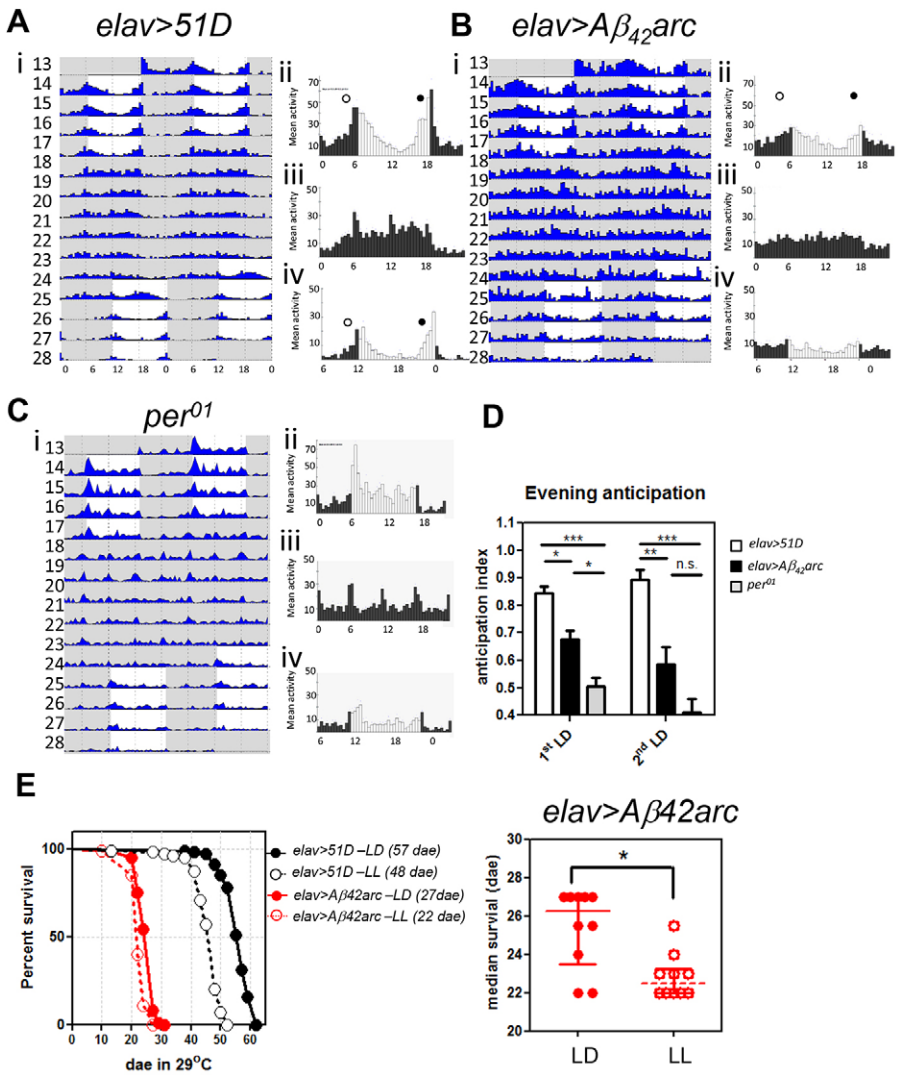

Fig. 2. Arrhythmia in Aβ$_{42}$arc-expressing flies is not reversible by LD cycles. (Ai) Average actogram of control flies (age 14 dae, *n*=16) undergoing 4 days LD, 6 days DD and followed by a 6-hour phase-shifted LD for 4 days. Two continuous days are plotted in each row (day *n* on the left and day *n*+1 on the right; i.e. day *n*+1 in row 13 is equivalent to day *n* in row 14), in which the *y*-axis is activity in each day and *x*-axis is the hours in each day; the grey shaded area marks the dark phases. Numbers 13-28 represent dae under recording. (Aii-iv) The average daily activity histogram for the first 4 days LD (ii), 6 days DD (iii) and the final 4 days LD (iv) are plotted. Black bars: dark phase; white bars: light phase; morning ramping: white circles; evening ramping: black circles. (B) The average actogram (i) and histograms (ii-iv) of arrhythmic *elav>Aβ$_{42}$arc* flies (age 14 dae and arrhythmic during DD, *n*=19). (C) *per^{01}* flies are used as negative controls, showing no anticipation. (D) Quantification of the evening anticipatory activity (mean ± s.e.m.) for the first LD and second LD shown in A-C by anticipatory index (the total activity 3 hours before darkness/the total activity 6 hours before darkness). Asterisks: significant difference by non-parametric one-way ANOVA (***P<0.001; **P<0.01; *P<0.05; n.s.: not significant). (E) Left panel: survival curves under LD (solid line) or LL (dashed lines) for *elav>Aβ$_{42}$arc* (red line) or *elav>51D* (black line) flies. The estimated median survivals (dae) from 100 individuals in each genotype are indicated in brackets. Flies in LL die significantly sooner that those in LD (P<0.001, log-rank test) in both *elav>51D* and *elav>Aβ$_{42}$arc*. Right panel: a more conservative measure in median survival is calculated from the ten sets of ten *elav>Aβ$_{42}$arc* flies in LD (filled circle) and LL (blank circles). Bars indicate median and first and third quartiles. Asterisk: significance determined by non-parametric Student's *t*-test (P<0.05).

continuous light (LL) conditions. Consistent with a previous study (Pittendrigh and Minis, 1972), there was a significant reduction in the lifespan for control flies in LL (48 dae *elav>51D*, Fig. 2E) as compared with LD (57 dae, *elav>51D*, P<0.001, log-rank test, n=100, as 10 sets of 10 flies, for each condition, 18% increase over LL, Fig. 2E). Remarkably, Aβ$_{42}$arc-expressing flies benefited identically from LD despite their arrhythmic behaviour (*elav>Aβ$_{42}$arc*, LL: 22 dae vs LD: 27 dae, P<0.001, log-rank test, n=100 for each conditions, 18% increase over LL and P<0.05; Student's *t*-test, 10 sets of 10 flies, Fig. 2E). Because LL conditions disrupt both behavioural and molecular circadian oscillations in flies (Konopka et al., 1989; Marrus et al., 1996), the observed increase in lifespan on going from LL to LD might be the result of residual clock functions in *elav>Aβ$_{42}$arc* flies despite their behavioural arrhythmicity.

The central molecular clock continues to oscillate in Aβ-expressing flies

We used two approaches to test, at both the cellular and molecular levels, whether the central clock apparatus remains intact during the progression of Aβ toxicity even though the flies exhibit arrhythmic behaviour. The first approach involved the direct visualisation of the structural integrity of a subgroup of clock neurons (PDF-positive cells) that are essential for maintaining intrinsic rhythmicity in DD (scheme of clock neurons, Fig. 3A) (Renn et al., 1999). When we compared control flies and Aβ$_{42}$arc-expressing flies by counting the number of PDF-positive cell bodies, we found no differences at least until 30 dae (Fig. 3B). We also visualised two dorsal neuronal groups – LNds and DN1s – by staining for Period (Per) protein. Again, we found no evidence of clock neuron loss in *elav>Aβ$_{42}$arc* flies as compared with controls (Fig. 3C,D). Additionally, there was no correlation between the Aβ-plaque density and the number of clock neurons in *elav>Aβ$_{42}$arc* fly brains (supplementary material Fig. S1G). Despite the absence of gross structural changes in the clock neurons, we employed a second approach to look for functional deterioration. By measuring the bioluminescence derived from a Per-luciferase fusion construct, *8.0-luc:9* (Veleri et al., 2003), we were able to monitor the molecular clock as it pertains to Per protein oscillation. Previous work has indicated that the *8.0-luc:9* strain faithfully reports molecular clock oscillations in non-PDF dorsal clock neurons (DNs and LNds) in the fly brain (Hodge and Stanewsky, 2008; Sekine et al., 2008; Sehadova et al., 2009). Comparing *8.0-luc:9/elav>Aβ$_{42}$arc* flies with equivalent control flies that do not express Aβ (Fig. 3E), we found that the rhythmic robustness of the bioluminescence was the same for both populations. To confirm that the bioluminescence from the Per-luciferase fusion construct was correctly reporting the oscillation

Disease Models & Mechanisms (2014) doi:10.1242/dmm.014134

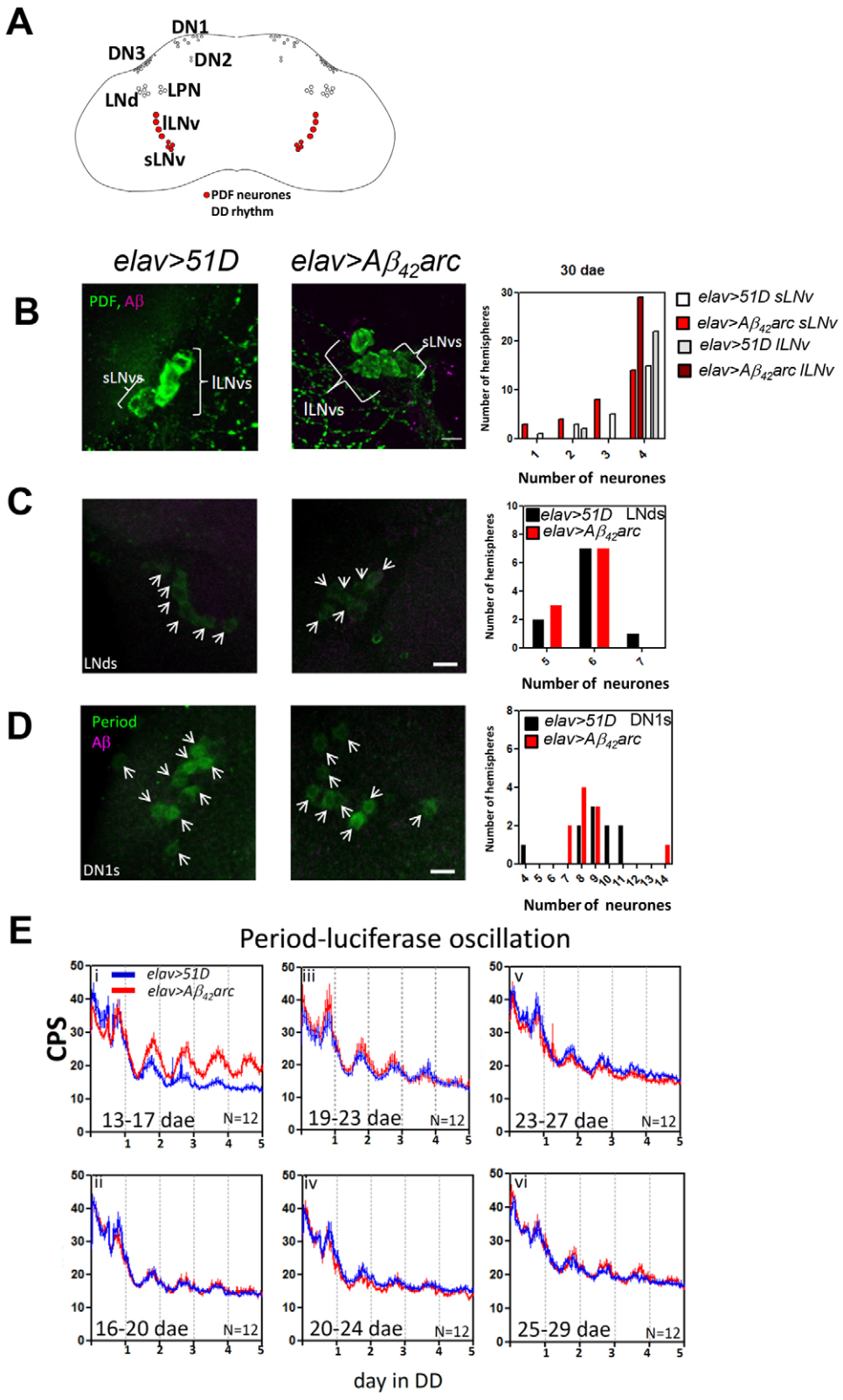

Fig. 3. Intact central molecular clock in *elav>Aβ$_{42}$arc* flies. (A) Scheme showing the 150 central clock neurons divided into seven groups. Red circles: PDF neurons, essential for DD rhythm. (B) Left panels: immunostaining of PDF neurons (sLNvs and lLNvs; green) and Aβ (magenta) for control *elav>51D* and *elav>Aβ$_{42}$arc* flies. Right panels: no difference (determined by χ^2-test) was found in the number of PDF neurons between *elav>Aβ$_{42}$arc* (*n*=29 brain hemispheres) and control *elav>51D* (*n*=24) flies. (C,D) Dorsal clock neurons, LNds (C) and DN1s (D), are identified by Period (Per)-positive staining (green) and anatomical localisation (arrows) for 30-dae-old *elav>51D* and *elav>Aβ$_{42}$arc* flies. No difference (by χ^2-test) in the number of LNd and DN1 neurons were found between *elav>Aβ$_{42}$arc* (*n*=15, 30 dae) and control *elav>51D* (*n*=13, 30 dae). Magenta: Aβ peptide. Scale bars: 10 µm. (E) None of the pairwise differences between amplitudes of *8.0-luc:9* profiles in *elav>Aβ$_{42}$arc* flies (red, mean ± s.e.m.) and that in *elav>51D* controls (blue, mean ± s.e.m.) are significant at indicated age groups (see supplementary material Table S1 for detailed statistics). As the experiment was designed as continuous sets of overlapping 5-day windows on *8.0-luc:9* luciferase activity profile, Kruskal-Wallis ANOVA statistics (with Dunn's Multiple Comparison post-test), instead of multiple *t*-test, are used to account for variation and to determine the significance of differences in amplitude as compared with age-matched controls. Numbers of flies are indicated (N). CPS, counts per second.

of Per protein, we immunostained the brains of control and *Aβ$_{42}$arc*-expressing flies for Per at various times during the second day of constant darkness post-entrainment. By specifically assessing the intensity of Per staining in the clock neurons (DN1s, LNds and sLNvs) we could confirm that the behaviourally arrhythmic *Aβ$_{42}$arc*-expressing flies exhibited the same diurnal Per oscillation as we see in control flies (green staining, supplementary material Fig. S2). By contrast, there was no circadian variation in the density of the Aβ peptide deposits (magenta, supplementary material Fig. S3A).

Taken together, these data indicate that the circadian behavioural abnormalities seen in Aβ-expressing flies are not caused by loss of

Disease Models & Mechanisms (2014) doi:10.1242/dmm.014134

central molecular clock function but are more likely due to damage in the downstream pathways in the clock neurons or other distal brain region.

$A\beta_{42}$ expression in clock cells is insufficient to cause circadian arrhythmicity

Although these results underline the importance of Aβ-mediated degradation of the clock output pathways, the studies showing cell loss in the SCN in AD postmortem samples indicate that damage to the central clock neurons is a possible cause for circadian rhythm deficits (Wu and Swaab, 2007). For this reason we were interested to know how the flies would respond to a range of Aβ insults that were restricted to the clock system. To this end we used the driver lines *timeless-gal4*, which drives expression in all clock cells including neurons and glia (Fig. 4A), and *pdf-gal4*, which drives expression in PDF-positive clock neurons (Kaneko and Hall, 2000). As with *elav-gal4*, the clock-neuron-specific expression of the less-aggregation-prone Aβ isoforms $A\beta_{40}$ and $A\beta_{42}$ had few or no behavioural consequences. Surprisingly, both *pdf>*$A\beta_{42}$*arc* and *tim>*$A\beta_{42}$*arc* expression exhibited robust behaviour; this is in contrast to the arrhythmicity induced when $A\beta_{42}$arc was expressed ubiquitously (cf. Fig. 4Bi,Ci and Fig. 1A). To test the possibility that the absence of any phenotype is due to lower expression levels for *pdf* and *tim* lines, as compared to *elav*, we measured gal4-dependent expression of GFP as a control. When we quantified GFP fluorescence specifically in PDF-positive neurons we found that the expression levels were essentially identical for all three (*elav*, *pdf* and *tim*) drivers (arrows in supplementary material Fig. S4A,B and quantification in S4C). The only remarkable difference was that, for *elav*-driven expression, the levels of GFP in the bulk of the brain (that is the non-clock neurons) were higher, as expected (supplementary material Fig. S4D). Taken together, these data indicate that Aβ expression that is restricted to clock cells is insufficient to trigger circadian abnormalities.

More focused expression of Aβ in clock neurons promotes further resistance to circadian arrhythmia

Although $A\beta_{42}$arc expression in clock cells was compatible with normal circadian behaviour, we tested whether the highly toxic tandem $A\beta_{42}$ construct ($TA\beta_{42}$) could induce arrhythmia under similar conditions. $TA\beta_{42}$ consists of two repeats of the $A\beta_{42}$ sequence linked by a glycine-rich 12mer linker peptide. We have previously shown that $TA\beta_{42}$ has an oligomer-rich aggregation mechanism (Speretta et al., 2012) and indeed *elav*-driven expression at 25°C results in developmental lethality (data not shown). By

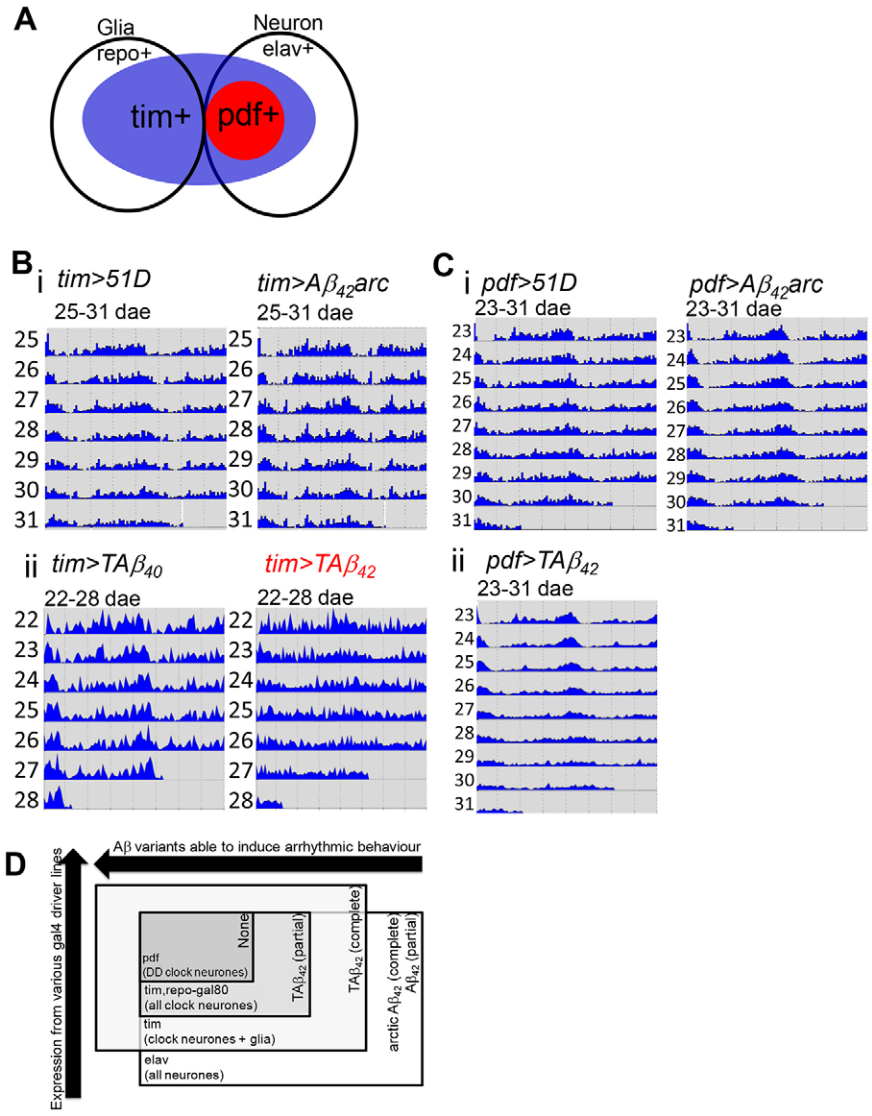

Fig. 4. Clock neurons are relatively resistant to $A\beta_{42}$ toxicity. (A) Scheme showing *gal4* and *gal80* transgene expression in *elav-gal4* (elav+, all neurons), *pdf-gal4* (pdf+, red, PDF-positive neurons) and *tim-gal4* (tim+, blue, including neurons and glia) driver lines, and *repo-gal80* (repo+, all glia) and *pdf-gal80* (pdf+, red, PDF positive neurons) repressor lines in the *Drosophila* nervous system. (Bi,Ci) Average actograms showing normal DD rhythms in *tim>*$A\beta_{42}$*arc* (*n*=16, 25-31 dae) and *pdf>*$A\beta_{42}$*arc* (*n*=16, 23-31 dae) as compared with *tim>51D* (*n*=16, 25-31 dae) and *pdf>51D* (*n*=15, 23-31 dae). (Bii,Cii) Average actograms showing arrhythmic DD behaviour in *tim>*$TA\beta_{42}$ (*n*=12, 22-28 dae) and normal rhythm in *pdf>*$TA\beta_{42}$ (*n*=11, 23-31 dae) as compared to control *tim>*$TA\beta_{40}$ (*n*=8, 22-28 dae) and *pdf>51D* (i, *n*=15, 23-31 dae; see Ci). See Table 1 for the total number of flies tested. (D) Scheme summarising that circadian arrhythmia derived from $A\beta_{42}$ expression within various extent centred on clock neurons in relation to two factors: the $A\beta_{42}$ species required for causing behavioural arrhythmia (horizontal: right to left including $A\beta_{42}$, $A\beta_{42}$arc and $TA\beta_{42}$ species) and the extent of $A\beta_{42}$ expression (vertical, bottom to top with more restricted expression). PDF neurons (dark grey rectangle) and all clock neurons (light grey rectangle) are more resistant to $A\beta_{42}$ insults, because $TA\beta_{42}$ triggers no (dark grey rectangle) or intermediate (light grey rectangle) circadian arrhythmia, whereas $TA\beta_{42}$ in all clock cells and $A\beta_{42}$arc expression in all neurons is enough to cause complete arrhythmia (white rectangle).

Disease Models & Mechanisms (2014) doi:10.1242/dmm.014134

contrast, the TAβ$_{40}$ variant, although equally aggregation prone, does not form oligomers and is essentially non-toxic (Speretta et al., 2012). When TAβ$_{42}$ was expressed in all clock cells using the *tim* driver, we observed significant arrhythmic behaviour as compared with *tim>Aβ$_{42}$arc* and non-Aβ controls (ages between 10 dae and 32 dae; Table 1 and Fig. 4Bii). Further restriction in the scope of TAβ$_{42}$ expression was achieved by using *repo-gal80* to suppress expression in the glial subset of tim-positive cells (*tim,repo-gal80*,

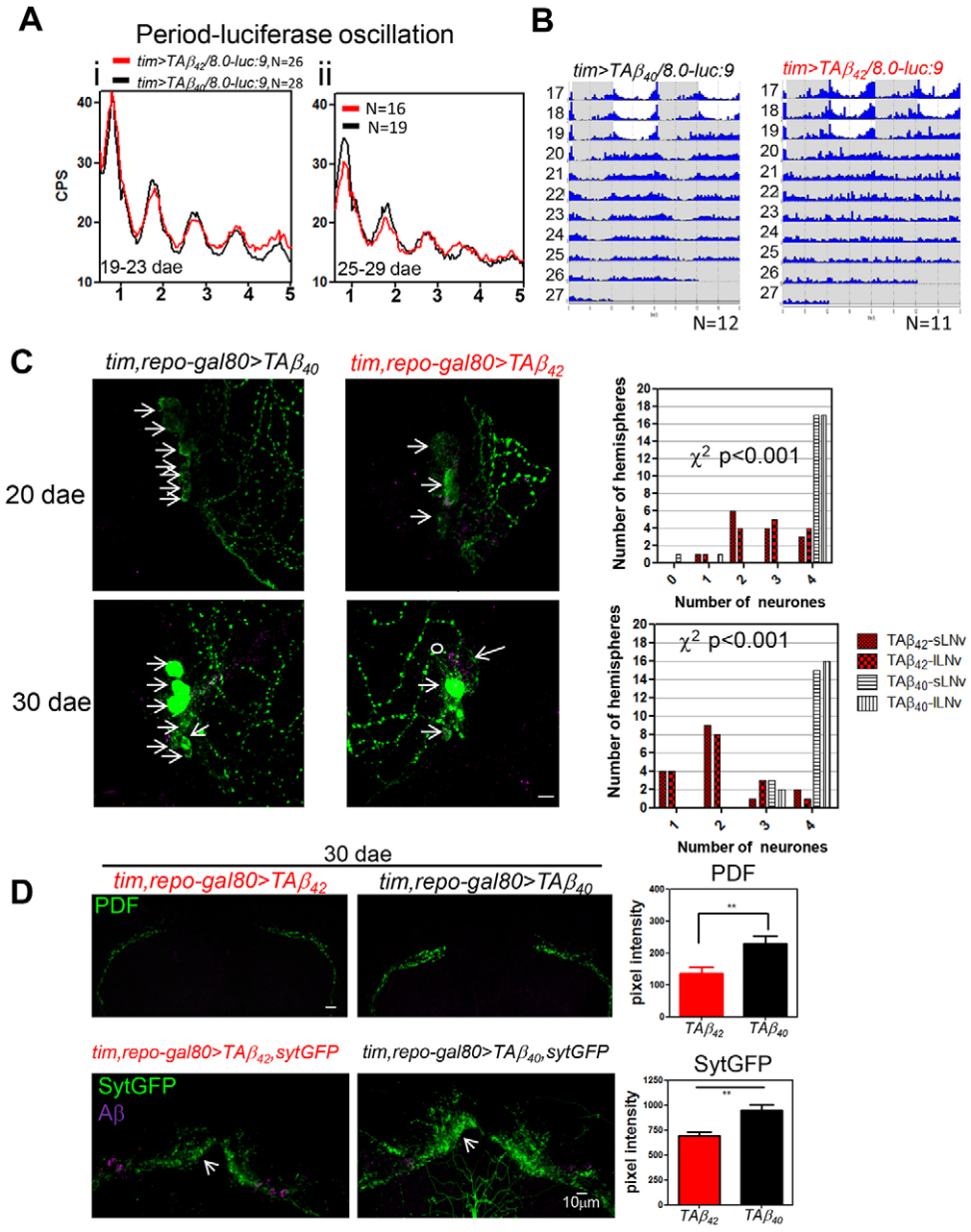

Fig. 5. TAβ$_{42}$ expression results in dysfunction and loss of clock neurons and has a minor effect on the remaining molecular clock. (A) Similar bioluminescence profiles (Per-luciferase fusion, *8.0-luc:9*) are found for *tim>TAβ$_{42}$/8.0-luc:9* (red, average trace) and control *tim>TAβ$_{40}$/8.0-luc:9* (black, average trace) between ages 19 dae to 29 dae. The profiles represent data merged from several flies (*n* from 16 to 28 per experiment). CPS, counts per second. (B) Average actograms for *tim>TAβ$_{42}$/8.0-luc:9* (arrhythmic) and control *tim>TAβ$_{40}$/8.0-luc:9* flies. Two continuous days are plotted in each row (day *n* on the left and day *n*+1 on the right; i.e. day *n*+1 in row 17 is equivalent to day *n* in row 18), in which the *y*-axis is activity in each day and *x*-axis is the hours in each day; the grey shaded area marks the dark phases. Numbers 17-27 represent dae in recording. (C) Image stacks showing that fewer PDF neurons (green and arrows) coincided with Aβ-positive staining (magenta and circle) in *tim,repo-gal80>TAβ$_{42}$* fly brains as compared with those in *tim,repo-gal80>TAβ$_{40}$* flies at the indicated age groups. Significant differences (χ^2-test) in the number of sLNv and lLNvs were found between the two genotypes (P<0.001). Number of hemispheres *n*=16 for 30 dae, *tim,repo-gal80>TAβ$_{42}$*; *n*=18 for 30 dae, *tim,repo-gal80>TAβ$_{40}$*; *n*=14 for 20 dae, *tim,repo-gal80>TAβ$_{42}$*; *n*=18 for 20 dae, *tim,repo-gal80>TAβ$_{40}$*. (D) Top panels: image stacks demonstrating reduced PDF peptide signal (green) at dorsal termini of sLNvs in 30-dae-old *tim,repo-gal80>TAβ$_{42}$* fly brain as compared with controls. The PDF signals in *tim,repo-gal80>TAβ$_{42}$* (red bars, mean ± s.e.m.) are significantly lower than that in *tim,repo-gal80>TAβ$_{40}$* (black bars, mean ± s.e.m., $^{**}P$<0.01, Student's *t*-test). Number of hemispheres (*n*)=16 for *tim,repo-gal80>TAβ$_{42}$*; *n*=18 for *tim,repo-gal80>TAβ$_{40}$*. Lower panel: dorsal output axonal terminal (arrows) of clock neurons is marked by synaptotagmin-GFP (sytGFP, green). Significant reduction in sytGFP signal in 30-dae-old *tim,repo-gal80>TAβ$_{42}$,sytGFP* flies (red bars, mean ± s.e.m.) was observed as compared with *tim,repo-gal80>TAβ$_{40}$,sytGFP* controls (black bars, mean ± s.e.m.) at ZT3 ($^{**}P$<0.01, Student's *t*-test). ZT denotes zeitgeber time with ZT0 indicating dawn and ZT12 dusk during LD cycles. *n*=14, *tim,repo-gal80>TAβ$_{42}$,sytGFP*; 8, *tim,repo-gal80>TAβ$_{40}$,sytGFP*. Aβ signal (magenta). Scale bars: 10 μm.

Disease Models & Mechanisms (2014) doi:10.1242/dmm.014134

supplementary material Fig. S5; Fig. 4A). Although more rhythmic than the *tim>TAβ42* flies at the same age, *tim,repo-gal80>TAβ42* flies showed a reduced rhythmic percentage and reduced rhythmicity as compared to controls (supplementary material Fig. S5B) without any potentially confounding decrease in average locomotor activity (supplementary material Fig. S5C). Remarkably, even TAβ42, when driven by *pdf-gal4*, was insufficient to induce arrhythmic behaviour (Fig. 4Cii; Table 1), indicating that the roles of Aβ expression outside PDF neurons are likely to be of primary importance. Moreover, cell-autonomous effects of Aβ are likely to be a relatively minor contributor to circadian abnormalities (Fig. 4D).

The molecular clock continues to oscillate until the neurons die

The preceding data indicate that pan-clock expression, driven by *tim-gal4*, is the most clock-restricted domain that generates robust TAβ42-mediated circadian arrhythmia. To assess the functional and structural integrity of the clock system under these conditions we again employed a number of molecular and cellular techniques. In *tim>8.0-luc:9/TAβ42* flies, aged between 19 dae and 29 dae, we found that the central molecular clock retained its rhythmicity (Fig. 5A) despite the behavioural arrhythmia and significant clock-cell loss induced by expression of TAβ42 (Fig. 5B; supplementary material Fig. S6). A similar pattern of behavioural arrhythmia and cell loss was observed when TAβ42 was restricted to clock neurons (*tim,repo-gal80>TAβ42*, Fig. 5C; supplementary material Fig. S5).

We also studied Aβ42-linked synaptic dysfunction in clock neurons in two ways using confocal microscopy; firstly, we immunostained the brains for the PDF peptide, as a marker of PDF-positive clock neurons, and, secondly, we assessed the intensity of a chimaeric GFP-synaptotagmin construct that accumulates presynaptically in all clock neurons. In both cases we quantified the signal intensity at the dorsal termini, a major site of clock neuron axonal projection. We found that the presence of TAβ42 markedly reduced PDF peptide and GFP signals in these areas, indicating a paracrine abnormality in PDF neurons and presynaptic dysfunction in clock neurons (Fig. 5D). Given the relatively robust character of the molecular clock signal in the face of extensive neuronal dysfunction, and appreciable neuronal death, it seems likely that the central molecular clock continues to 'tick' until the cells die and are physically lost. In other words, the molecular clock seems to be the most robust feature of the clock system during Aβ pathology, being interrupted only by neuronal dysfunction and death.

Non-cell-autonomous Aβ toxicity

So far we have demonstrated that even TAβ42 does not induce arrhythmia when expressed exclusively in PDF neurons (Fig. 6Ai); by contrast, use of a *tim-gal4* driver that includes glia, pdf neurons and other nearby clock neurons does cause arrhythmia (Fig. 6Aii). Therefore, we were interested to determine whether the behavioural disturbance consequent on the expression of Aβ is mediated by cell-autonomous mechanisms, or not. To achieve the expression of TAβ42 throughout the clock system but specifically not in the PDF-positive neurons that control the DD rhythm (Fig. 6Aiii), we used the *tim,pdf-gal80* driver. In this experiment we find that, although the number of PDF neurons is not affected by the expression of TAβ42, we do see a reduction in PDF peptide staining in the dorsal terminus of PDF-positive neurons (Fig. 6B). The hypothesis that PDF neurons are dysfunctional, despite not expressing Aβ themselves, was justified by the finding that the flies also exhibited behavioural arrhythmia in DD (Table 1).

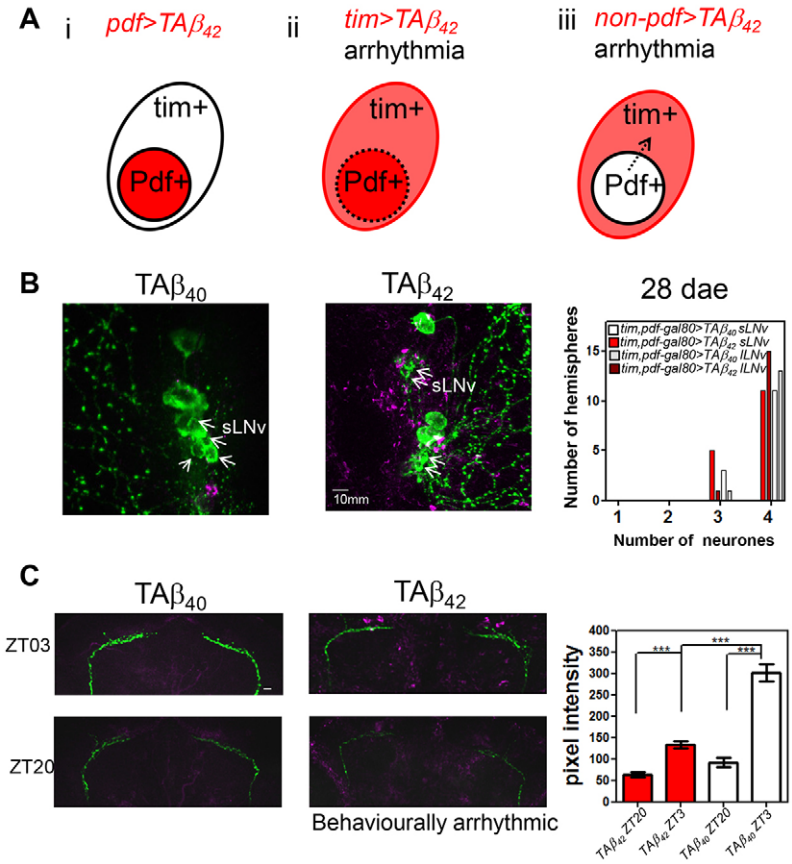

Fig. 6. TAβ42-mediated non-cell-autonomous toxicity to PDF neurons. (A) Schemes showing that: (i) expression of TAβ42 (red area, *pdf>TAβ42*) in only PDF neurons results in no circadian abnormality up to 30 dae; (ii) expression of TAβ42 in all clock cells (red and pink areas, *tim>TAβ42*) results in circadian arrhythmia and loss of PDF neurons (marked by dashed outline of PDF neurons); (iii) expression of TAβ42 exclusively in clock cells except for PDF neurons (pink area, *non-pdf>TAβ42*) results in no neuronal loss but reduced PDF peptide signal (dashed arrow) in PDF neurons. (B) Left panels: representative images demonstrating no PDF neuronal loss (green) in *tim,pdf-gal80>TAβ42* as compared with control *tim,pdf-gal80>TAβ40*. Aβ plaques are detected in *tim,pdf-gal80>TAβ42* fly brains (magenta). No difference in the number of PDF neurons for both sLNvs (arrows) and lLNvs was detected between 28-dae *tim,pdf-gal80>TAβ42* and *tim,pdf-gal80>TAβ40* (see graph on right). Significance was determined by χ^2-test. See Table 1 for reduced behavioural rhythmicity in *tim,pdf-gal80>TAβ42*. (C) Left panels: representative image stacks demonstrating reduced PDF peptide signal at dorsal termini of sLNvs in *tim,pdf-gal80>TAβ42* fly brain as compared with controls at indicated time points during LD cycles. ZT denotes zeitgeber time with ZT0 indicating dawn and ZT12 dusk during LD cycles. Right panels: PDF signals in *tim,pdf-gal80>TAβ42* (red bars, mean ± s.e.m.) are significantly lower than that in *tim,pdf-gal80>TAβ40* (white bars, mean ± s.e.m.) at ZT3 (***P<0.001, one-way ANOVA). Although both genotypes maintain the daily oscillation of PDF peptide signal (ZT3 vs ZT20, ***P<0.001, one-way ANOVA), no oscillation of Aβ plaque density was detected (see supplementary material Fig. S3B). n=16, *tim,pdf-gal80>TAβ42*; 14, *tim,pdf-gal80>TAβ40*. Scale bar: 10 μm.

DISCUSSION

Pan-neuronal Aβ expression causes circadian arrhythmia

The dampening, and eventual disintegration, of circadian behaviour in individuals with AD constitutes one of the most distressing clinical features of the disorder. Although there is evidence that cell loss in the SCN is correlated with such symptoms of AD, it is not known whether damage to the molecular clock, the clock neurons, or rather to the output pathway, underpins the behavioural deficits. To address these questions we have expressed Aβ peptides pan-neuronally in the fly brain and assessed the consequences for circadian behaviour. During the lifespan of our flies, we found that pan-neuronal $A\beta_{40}$ and $A\beta_{42}$ expression had no effect on circadian locomotor behaviour. By contrast, expressing the Arctic variant of $A\beta_{42}$ ($A\beta_{42}$arc) resulted in profound age-dependent behavioural arrhythmia as evidenced by a progressively increasing arrhythmic sub-population, reduced overall rhythm robustness in DD (Fig. 1) and loss of anticipatory activity in LD (Fig. 2), recapitulating the dampening of behavioural rhythms in individuals with AD (Volicer et al., 2001) and demonstrating a loss of circadian regulation that could be considered as the fly equivalent of 'sundowning' (Fig. 2D). Flies were not aged past 35 days because thereafter control flies exhibit circadian abnormalities (Rezával et al., 2008; Luo et al., 2012; Rakshit et al., 2012; Umezaki et al., 2012) and the differences between Aβ-expressing and control flies become less clear.

The more marked consequences of $A\beta_{42}$arc expression are thought to be due to the increased aggregation propensity of this peptide and to its oligomer-rich aggregation mechanism (Nilsberth et al., 2001; Whalen et al., 2005; Luheshi et al., 2007). Our previous studies have shown that the fly reports the presence of such oligomeric aggregates and these species correlate more closely with climbing and longevity deficits than do large insoluble aggregates (Luheshi et al., 2007; Speretta et al., 2012). Likewise, the circadian behavioural abnormalities demonstrated here also correlate more closely with oligomer formation ($A\beta_{40} \leq TA\beta_{40} \leq A\beta_{42} < A\beta_{42}arc < TA\beta_{42}$, see Figs 1 and 4) than they do with total Aβ plaque density in the fly brains (supplementary material Fig. S1). Therefore, we reason that oligomeric species instead of large aggregates are the likely cause of the circadian deficits. These findings are concordant with similar experiments in the mouse, where animals expressing a disease-linked APP mutation, with or without mutant PS1 and tau, were found to retain essentially normal DD circadian behaviour throughout life (Wisor et al., 2005; Sterniczuk et al., 2010). Because these mice represent a model of wild-type $A\beta_{42}$ overproduction, this might explain why, like in the *elav>Aβ42* flies, little or no circadian abnormality was observed (Table 1). It is possible that increasing the levels of oligomeric aggregates, by introducing additional copies of the wild-type $A\beta_{42}$ transgene, or by ageing the flies for longer, might also elicit circadian abnormalities. However, as it stands, our fly model of $A\beta_{42}$arc toxicity is the first experimental animal that robustly recapitulates the progressive circadian deficits found in AD.

Behavioural arrhythmia is not due to disruption of the molecular clock

One of the remarkable conclusions of our study is that central clock neurons survive and continue to exhibit circadian oscillation of at least one clock-related protein in the face of Aβ-induced behavioural arrhythmia. This was most apparent in flies expressing pan-neuronal arctic $A\beta_{42}$ ($A\beta_{42}$arc). Despite exhibiting locomotor arrhythmia from ~12 dae, these flies had morphologically normal central clock neurons until at least 30 dae. Specifically, the PDF-positive sLNv neurons, which are essential for DD rhythmicity, remained intact. Furthermore, the non-PDF clock neurons continued to express the Per-luciferase reporter construct (*8.0-luc:9*) in a circadian pattern that was essentially identical to rhythmic control flies (Fig. 3E). Concordant with this finding, immunostaining of Per protein in $A\beta_{42}$arc-expressing flies also confirmed its normal circadian oscillation in clock neurons during constant darkness and despite Aβ-induced arrhythmia (in DN1s, LNds and sLNvs; supplementary material Fig. S2). When we subsequently restricted the neuronal expression of Aβ to the clock system using *tim-gal4* we observed equivalent behavioural arrhythmia; however, in this context, $A\beta_{42}$arc was insufficiently potent. Instead, the highly toxic tandem $A\beta_{42}$ construct was required to induce arrhythmia and was accompanied by some loss of both sLNv and ILNv neurons. Despite the expression of this highly toxic Aβ construct, and the consequent loss of PDF neurons, the molecular oscillations in dorsal clock neurons continued unabated (Fig. 5). Taken together, our data indicate that cell-autonomous Aβ toxicity is insufficient to disrupt the oscillation of the central molecular clock.

$A\beta_{42}$ expression in clock neurons is insufficient to cause circadian arrhythmicity

Notable was the lack of a circadian phenotype even when we expressed the highly toxic $TA\beta_{42}$ in PDF neurons alone. Indeed, the resistance of the PDF neurons to $A\beta_{42}$ expression has been remarked upon in passing by others (DiAngelo et al., 2011). When we expanded the expression of $TA\beta_{42}$ to include all clock neurons, by using *tim,repo-gal80*, the flies became behaviourally arrhythmic. Indeed, further expansion to also include tim-positive glial cells (using *tim-gal4*), resulted in a progressive circadian degradation in $TA\beta_{42}$ flies and so supports a role for glia in modulating clock neuronal activity (Ng et al., 2011). Such evidence highlights the contribution of circuits peripheral to the central clock neurons in mediating Aβ-linked circadian locomotor deficits, particularly in the ageing brain (Nakamura et al., 2011; Luo et al., 2012).

Our conclusions are concordant with Pallier and colleagues, who studied the R6/2 Huntingdon's disease (HD) mouse (Pallier et al., 2007) and found that a Per-luciferase reporter continued to oscillate in *ex vivo* SCN preparations despite the behavioural arrhythmia of the donor animals. These investigators, like us, concluded that the primary target for circadian disruption in the R6/2 mouse is external to the central pacemaker. Such parallels between AD and HD models indicate that damage to the communication between central pacemaker neurons and other neuronal circuits might be a pathological feature that is common to neurodegenerative disorders. In the human context, the central clock neurons in the SCN are thought to use the pineal gland as one of their downstream targets; in this regard it is interesting to note that one consequence of AD is that the secretion of melatonin from the pineal becomes arrhythmic (Wu et al., 2006).

The axons of the clock neurons are a target for Aβ toxicity

The manifestation of circadian locomotor rhythmicity in the fly requires the synchronisation of the molecular clocks in central clock neurons, downstream neurons and in the peripheral tissues. All this is thought to be dependent on both peptidergic paracrine and synaptic communication. Our work has particularly implicated dysfunction in the dorsal protocerebrum as an important pathological mechanism, on the basis of reduced PDF staining and synaptotagmin-GFP (sytGFP) intensities in this area (Fig. 5D). When determining the mechanisms underlying Aβ toxicity on pacemaker PDF neurons, we have demonstrated that PDF peptide signal is reduced by expressing Aβ not in PDF neurons themselves but in neighbouring cells that are in communication with PDF

neurons (i.e. *tim,pdf-gal80>TAβ42*, Fig. 6Aiii). Such non-cell-autonomous toxicity of Aβ has long been suspected (Busche et al., 2008); however, to our knowledge, this is the first *in vivo* demonstration of toxicity in one neuron as a consequence of Aβ being expressed explicitly by its neighbours. Considering the importance of PDF peptides in synchronising clock neurons under DD conditions, such reduced PDF signals likely contribute to the behavioural arrhythmia in *tim,pdf-gal80>TAβ42* flies. Furthermore, the cell-autonomous toxicity of Aβ on PDF neurons likely had no role in generating these circadian phenotypes (Fig. 6A).

Nevertheless, Aβ-mediated arrhythmia cannot be equated to a pure loss of the PDF signal, because killing PDF neurons by expressing hid (*pdf>hid*, Table 1) results in characteristic short period rhythms in the remaining rhythmic subpopulation, something that we do not see in any of our Aβ-expressing flies. Notably, the behavioural abnormalities in *tim>TAβ42* and *tim,pdf-gal80>TAβ42* flies resembles the phenotype of *tim>tetanus-toxin*, in which synaptic blockade results in arrhythmic flies despite an intact molecular clock (Kaneko et al., 2000). In summary, our findings signify Aβ-mediated damage to both axonal outputs and paracrine signalling in clock neurons.

An entrained central clock benefits the organism despite behavioural arrhythmia

It has previously been documented that animals in a rhythmic LD environment live longer than those exposed to rhythm-disrupting light cycles (Pittendrigh and Minis, 1972; Davidson et al., 2006; Park et al., 2012). Similarly, loss of normal circadian behaviour in humans is associated with increased morbidity and mortality (Paudel et al., 2010; Tranah et al., 2011). Of particular interest recently has been the finding that behavioural and molecular arrhythmia in per^{01} flies is accompanied by increased oxidative stress (Krishnan et al., 2012) and this could increase neurotoxicity in AD (Rival et al., 2009). However, it is unclear whether it is the circadian behaviour pattern per se, or alternatively an entrained molecular clock, that prolongs life. In this regard we have made the interesting observation that profoundly arrhythmic $Aβ_{42}$arc flies live longer when exposed to LD as compared to those in the clock-disrupting LL environment. Indeed, the proportional increase in median survival is identical for both control and arrhythmic Aβ flies on going from LL to LD. In the absence of a visible behavioural correlate, it seems likely that an entrained molecular clock is beneficial and it is not the behavioural rhythms that prolong life.

Nevertheless, our data agree with the findings of Park and colleagues who concluded that the harmonious interaction of endogenous and environmental rhythms is optimal for longevity, something that was lost in their *per1per2* double-null mice (Park et al., 2012). Much is still unclear though; for example, we do not know whether entrainment needs to be central, or whether entrainment of one or more peripheral tissue clocks is sufficient. We can also speculate that the harmonious interplay of endogenous rhythms and behavioural activity might have an important role in protecting the organism from the oxidative stress that is a key feature of both arrhythmic organisms and individuals with AD. In particular, the circadian variation in antioxidant proteins such as peroxiredoxins (O'Neill et al., 2011; Edgar et al., 2012) might be timed to best protect the organism from the stress of oxidative cellular metabolism. Indeed it is notable that our arrhythmic Aβ-expressing flies show a general dampening in circadian behaviour, being moderately active throughout a 24-hour cycle. By contrast, per^{01} flies, which have a genetically impaired molecular clock, seem to respond to the light phase with activity and to dark with relative inactivity (Fig. 2Civ), being entirely arrhythmic only in continuous dark. Comparing the oxidative consequences of behavioural arrhythmia in these two contexts could provide interesting insights into pathogenesis of AD.

Nevertheless, these findings have implications for the environment that we provide for individuals with AD; indeed, it is already established that good circadian light hygiene can result in circadian behavioural improvements (Coogan et al., 2013). By contrast, our work has shown that, once Aβ-expressing flies became arrhythmic in a dark environment, light-dark cycling can no longer significantly restore circadian behaviour patterns. Despite this, our work has indicated that the benefits of a clean light-dark environment might not be expressed as improved behavioural end-points. Our research points to potentially disease-modifying benefits of an entrained molecular clock, possibly as a consequence of reduced oxidative damage, something that is known to characterise AD from its earliest stages (Nunomura et al., 2001; Markesbery et al., 2005).

MATERIALS AND METHODS

Fly strain and husbandry

All *gal4* and *gal80* lines expressing in the *Drosophila* clock system are gifts from Prof. Ralf Stanewsky (Queen Mary, London, UK), including *tim-gal4 (27)*, *tim-gal4 (62)*, *tim-gal4 (67)*, *tim-gal4 (86)*, *tim-gal4 (27),pdf-gal80* and *pdf-gal4* (Kaneko and Hall, 2000; Chen et al., 2011). Various *UAS-Aβ* lines, including *UAS-Aβ40*, *UAS-Aβ42*, *UAS-Aβ42arc*, *UAS-TAβ40* and *UAS-TAβ42*, were previously generated by the site-specific Phi31C system using acceptor line *51D* (therefore as the background control) and backcrossed to w^{1118} (Jahn et al., 2011; Speretta et al., 2012). The acceptor site is marked by RFP; however, we recently noticed that 20% of our w^{1118};*51D* line lost this signal during backcrossing. The pan-neuronal expression of Aβ is driven by *elav-gal4*^{c155} (Crowther et al., 2005). The fly strain, *tim,repo-gal80*, expressing Gal4 exclusively in *timeless* clock neurons, were generated by combining two transgenes: *tim-gal4 (67)* and *repo-gal80(N18)* (Awasaki et al., 2011). The *UAS-synaptotagmin-GFP* fly strain is a gift from Dr Cahir O'Kane (Department of Genetics, University of Cambridge). All the flies are reared in cornmeal food vials at 25°C and 70% humidity with continuous light-dark cycles (14 hour:10 hour).

Locomotor behaviour assay

The *Drosophila* circadian locomotor assay is adapted from that described previously (Chen et al., 2011). No more than 20 adult male flies of each genotype are aged in a cornmeal food, replaced every other day, before being transferred individually to a glass tube containing 2% w/v agar and 5% w/v sucrose. The age of the flies is expressed as the day after eclosion (dae) in this study. One-dimensional locomotor activity of each individual fly is then detected continuously by summing the beam crosses every 30 minutes in an automated infrared beam monitoring system (DAM system, Trikinetics, Waltham, USA). The DAM apparatus is placed in a temperature-regulated incubator (Model 200, LMS Ltd, UK), in which the light condition is regulated by a compact fluorescent lamp (660 lumen, Eveready, UK) controlled by an external 24-hour timer.

For detecting intrinsic circadian locomotor rhythm, flies at a given age are first entrained by 3 days of 12 hour:12 hour light-dark cycles (LD cycles) followed by 7 days of constant darkness (DD) at 25°C. The overall level of locomotor activity for individual flies was calculated by averaging the beam crosses/30 minutes over the 10-day duration of the experiment. The time-series of daily activity (actogram) for each fly is plotted and analysed using the Flytoolbox in MATLab software (Levine et al., 2002). The free-running period of the individual time-series under constant darkness is determined by an autocorrelation base method (Levine et al., 2002), in which the rhythmicity statistic (RS) value is derived as a measure of rhythmic robustness. The RS value is the ratio of the autocorrelation coefficient value of an activity time-series to its 95% confidence interval of sampling error (Levine et al., 2002). The mean and median of the RS values are calculated for all tested genotypes (Table 1). All flies with an RS value ≤1.5 are classed

as arrhythmic (Levine et al., 2002; Chen et al., 2011). The rhythmic percentage is the fraction of flies that achieve an RS >1.5. The mean and median of the period (hour) are calculated for each genotype from all rhythmic individuals. D'Agostino and Pearson omnibus normality test (GraphPad) was used to verify the normality of each dataset in this study before using parametric statistics; otherwise, non-parametric statistics have been applied. Non-parametric one-way ANOVA (Kruskal-Wallis with Dunn's comparison post-test) or Student's *t*-test are used to analyse differences in rhythmicity (RS) and the period between various genotypes and age groups (GraphPad software, Prism).

To assess whether LD rhythm can be re-entrained following DD, 14-dae *elav>Aβ$_{42}$arc* and *elav>51D* flies are first entrained by 4-day LD cycles, followed by 6 days of DD and a secondary series of four LD cycles with a 6-hour phase delay as compared with the primary LD. Flies with an RS value ≤1.5 are defined as arrhythmic during DD. The average actogram are plotted by Flytoolbox for all LD and DD sessions. In LD, the anticipatory activity ramps at dark-light (morning) and light-dark (evening) transitions are visualised using histograms plots. Quantification of the evening anticipation is chosen because of a clear difference in evening ramping activity between *elav>51D* flies and the arrhythmic *period*-null mutants (*per^{01}*) (see Stoleru et al., 2004) and also it is the fly equivalent of the 'sundowning' behaviour that is particularly significant for individuals with AD (Volicer et al., 2001). The anticipation quantification is based on Harrisingh/Individual Index (Harrisingh et al., 2007) by calculating the ratio of the total activity during the 3 hours before light-dark (evening) transitions to those in the 6 hours before the transitions for the first (2-4 day) and second (12-14 day) LD cycles.

Longevity assay

Flies containing UAS-Aβ variants are crossed with *elav-gal4^{c155}* driver lines. Female progeny are collected on the day of eclosion and mated for 24 hours before rearing in either 12-hour LD cycles or constant light (LL) at 29°C. The longevity was analysed as described previously (Crowther et al., 2005) with each assay being comprised of ten tubes of ten flies each (total 100 flies for each genotype). The statistical significance in median survival between LL and LD conditions was determined in two ways: (1) by using the estimates from the 100 individuals with the log-rank test (n=100) and, (2) more conservatively, by using the non-paired Student's *t*-test for ten population median survival derived from the ten tubes of ten flies for each conditions. Statistical significance was set at P<0.05.

Luciferase assay

Luciferase assays are modified from Chen et al. (Chen et al., 2011). Briefly, male flies expressing Per-luciferase protein fusion, *8.0-luc:9* (Veleri et al., 2003), and Aβ variants were generated from crossing *elav-gal4;8.0-luc:9* (this study) or *8.0-luc:9;tim-gal4* [obtained from Stanewsky (Hodge and Stanewsky, 2008)] to *UAS-Aβ* strains. Flies of each genotype are loaded in a white 96-well microtiter plate containing 5% w/v sucrose, 1% w/v agar and 15 mM luciferin (L-8220, Biosynth AG, Switzerland). Bioluminescence emitted from the flies was measured in a Packard Topcount Multiplate Scintillation Counter at 25°C for 2-3 days of LD before entering DD. Data were plotted and analysed using BRASS Version 2.1.3 (Locke et al., 2005). Fast Fourier transform-non-linear least squares (FFT-NLLS) was also performed by BRASS to estimate the period and the relative amplitude of each luciferase time-series. Relative amplitude error (Rel-amp error) values are used as a measure for rhythm robustness: if >0.7 then the individual luciferase activity would be assigned as arrhythmic (Stanewsky et al., 1997). Non-parametric one-way ANOVA are performed to analyse the significant difference (P<0.05) in the estimated period, amplitude and Rel-amp error among genotypes.

Confocal immunohistochemistry

The immunohistochemistry protocol is modified from that previously described (Hermann et al., 2012). After 3 days entrainment in LD conditions, male flies of each genotype at the given age were fixed at the indicated ZT and CT (defined below) in 4% w/v paraformaldehyde/PB0.1%T (0.1 M phosphate buffer, pH 7.4 with 0.1% v/v Triton X-100) at room temperature for 2.5 hours. ZT denotes zeitgeber time with ZT0 indicating dawn and ZT12 dusk during LD cycles. CT denotes constant time, with CT00 indicating subjective dawn and CT12 subjective dusk. After fixation, the samples are washed three times with PB at room temperature (RT). The whole brain was dissected out and blocked with 10% v/v goat serum in PB with 0.5% v/v Triton X-100 (PB0.5%T) for 2 hours at RT and stained with monoclonal mouse anti-PDF (1:1000, PDFC7, Developmental Studies Hybridoma Bank, USA) and polyclonal rabbit anti-Aβ$_{1\text{-}16}$ (1:500, SIG-39322, Covance) in PB0.5%T at 4°C for 48 hours. After washing six times in PB0.1%T, the samples are incubated at 4°C overnight with Alexa-Fluor-647-conjugated anti-rabbit and Alexa-Fluor-488-conjugated anti-mouse antibodies (Molecular Probes) diluted 1:300 in PB0.5%T. For Per and Aβ double staining (supplementary material Fig. S2), rabbit anti-Per (1:1000, gift from Ralf Stanewsky, QMUL) and monoclonal mouse anti-Aβ$_{1\text{-}16}$ (1:500, 6E10, Covance) are used and the secondary antibodies are Alexa-Fluor-647-conjugated anti-mouse and Alexa-Fluor-488-conjugated anti-rabbit (Molecular Probes). Brains were washed six times in PB0.1%T before being mounted in Vectashield. Samples were stored at 4°C until examination under a Nikon Eclipse C1si confocal microscope.

Quantification of confocal images

PDF neuron number

Image stacks are acquired along the anterior-posterior axis (*z*-axis) of the fly brain for each genotype from the confocal microscope with 40× magnification. ImageJ software was used to process and analyse all images. Large (lLNvs) and small (sLNvs) PDF neurons are identified by their anatomical location, size and PDF-peptide-positive staining. The number of the two neuron groups was counted separately per brain hemisphere (normally four per hemisphere of each neuronal group) (Helfrich-Förster et al., 2007) in the indicated genotype. The ratio of brain hemispheres with four PDF-positive neurons versus less than four was calculated. The significance of the differences was calculated using the χ^2-test in GraphPad Prism.

PDF peptide signal at the dorsal terminus

The brightest PDF signal in the dorsal terminus of sLNvs in individual brains was identified across the *z*-axis by tuning signal gain around saturation. A single confocal image was then taken below signal saturation with the same laser intensity and signal gain across all samples of the indicated genotypes. The PDF signal (S_{pdf}) was quantified by a ROI (region of interest) mask in ImageJ software. The same ROI mask was then moved to brain areas with no PDF signal to quantify the background signal (S_b), which was then subtracted from S_{pdf}. The average of S_{pdf} values, corrected in this way, was calculated for all individuals of the indicated genotypes and the difference among genotypes are determined by non-parametric one-way ANOVA.

GFP intensity

Image stacks containing PDF neurons are captured along the *z*-axis. The mean grey scale pixel intensities of GFP within PDF neurons were calculated by individual ROI circular masks outlined by the PDF-positive cell body (GFP_{pdf}). The average GFP signal in the observed brain area (GFP_b) for the indicated genotype was calculated from all the image stacks in a fixed field of view (318 μm^2). Both GFP_{pdf} and GFP_b signals were documented and compared among genotypes by non-parametric one-way ANOVA.

Acknowledgements

We thank Drs Ralf Stanewsky and Elena Carbognin for their helpful discussions and Drs Werner Wolfgang and Kalina Davies for their assistance with luciferase assays in SBCS, Queen Mary University of London. We thank Drs Ralf Stanewsky, Takeshi Awasaki, Sara Imarisio, Cahir O'Kane and Yuu Kimata for providing fly strains and equipment.

Competing interests

The authors declare no competing financial interests.

Author contributions

K.-F.C., B.P. and D.C.C. conceived and designed the experiments. K.-F.C. and B.P. performed the experiments. K.-F.C. analysed the data. B.P. and D.A.L. edited the paper and approved the final version of the manuscript. K-F.C. and D.C.C. wrote the paper.

Funding

This work was supported by the Wellcome Trust (D.C.C. and K.-F.C., grant code: 082604/2/07/Z) and Petrlik Foundation (B.P., Skidmore College). D.C.C. is an Alzheimer's Research UK Senior Research Fellow (grant code: ART-SRF2010-2).

Supplementary material

Supplementary material available online at
http://dmm.biologists.org/lookup/suppl/doi:10.1242/dmm.014134/-/DC1

References

Allada, R. and Chung, B. Y. (2010). Circadian organization of behavior and physiology in Drosophila. *Annu. Rev. Physiol.* **72**, 605-624.

Ambrée, O., Touma, C., Görtz, N., Keyvani, K., Paulus, W., Palme, R. and Sachser, N. (2006). Activity changes and marked stereotypic behavior precede Abeta pathology in TgCRND8 Alzheimer mice. *Neurobiol. Aging* **27**, 955-964.

Aton, S. J., Colwell, C. S., Harmar, A. J., Waschek, J. and Herzog, E. D. (2005). Vasoactive intestinal polypeptide mediates circadian rhythmicity and synchrony in mammalian clock neurons. *Nat. Neurosci.* **8**, 476-483.

Awasaki, T., Huang, Y., O'Connor, M. B. and Lee, T. (2011). Glia instruct developmental neuronal remodeling through TGF-β signaling. *Nat. Neurosci.* **14**, 821-823.

Blanchardon, E., Grima, B., Klarsfeld, A., Chélot, E., Hardin, P. E., Préat, T. and Rouyer, F. (2001). Defining the role of Drosophila lateral neurons in the control of circadian rhythms in motor activity and eclosion by targeted genetic ablation and PERIOD protein overexpression. *Eur. J. Neurosci.* **13**, 871-888.

Brand, A. H. and Perrimon, N. (1993). Targeted gene expression as a means of altering cell fates and generating dominant phenotypes. *Development* **118**, 401-415.

Brorsson, A.-C., Bolognesi, B., Tartaglia, G. G., Shammas, S. L., Favrin, G., Watson, I., Lomas, D. A., Chiti, F., Vendruscolo, M., Dobson, C. M. et al. (2010). Intrinsic determinants of neurotoxic aggregate formation by the amyloid β peptide. *Biophys. J.* **98**, 1677-1684.

Busche, M. A., Eichhoff, G., Adelsberger, H., Abramowski, D., Wiederhold, K.-H., Haass, C., Staufenbiel, M., Konnerth, A. and Garaschuk, O. (2008). Clusters of hyperactive neurons near amyloid plaques in a mouse model of Alzheimer's disease. *Science* **321**, 1686-1689.

Carmine-Simmen, K., Proctor, T., Tschäpe, J., Poeck, B., Triphan, T., Strauss, R. and Kretzschmar, D. (2009). Neurotoxic effects induced by the Drosophila amyloid-β peptide suggest a conserved toxic function. *Neurobiol. Dis.* **33**, 274-281.

Chen, K.-F., Peschel, N., Zavodska, R., Sehadova, H. and Stanewsky, R. (2011). QUASIMODO, a Novel GPI-anchored zona pellucida protein involved in light input to the Drosophila circadian clock. *Curr. Biol.* **21**, 719-729.

Coogan, A. N., Schutová, B., Husung, S., Furczyk, K., Baune, B. T., Kropp, P., Häßler, F. and Thome, J. (2013). The circadian system in Alzheimer's disease: disturbances, mechanisms, and opportunities. *Biol. Psychiatry* **74**, 333-339.

Crowther, D. C., Kinghorn, K. J., Miranda, E., Page, R., Curry, J. A., Duthie, F. A. I., Gubb, D. C. and Lomas, D. A. (2005). Intraneuronal Abeta, non-amyloid aggregates and neurodegeneration in a Drosophila model of Alzheimer's disease. *Neuroscience* **132**, 123-135.

Cusumano, P., Klarsfeld, A., Chélot, E., Picot, M., Richier, B. and Rouyer, F. (2009). PDF-modulated visual inputs and cryptochrome define diurnal behavior in Drosophila. *Nat. Neurosci.* **12**, 1431-1437.

Davidson, A. J., Sellix, M. T., Daniel, J., Yamazaki, S., Menaker, M. and Block, G. D. (2006). Chronic jet-lag increases mortality in aged mice. *Curr. Biol.* **16**, R914-R916.

DiAngelo, J. R., Erion, R., Crocker, A. and Sehgal, A. (2011). The central clock neurons regulate lipid storage in Drosophila. *PLoS ONE* **6**, e19921.

Duncan, M. J., Smith, J. T., Franklin, K. M., Beckett, T. L., Murphy, M. P., St Clair, D. K., Donohue, K. D., Striz, M. and O'Hara, B. F. (2012). Effects of aging and genotype on circadian rhythms, sleep, and clock gene expression in APPxPS1 knock-in mice, a model for Alzheimer's disease. *Exp. Neurol.* **236**, 249-258.

Edgar, R. S., Green, E. W., Zhao, Y., van Ooijen, G., Olmedo, M., Qin, X., Xu, Y., Pan, M., Valekunja, U. K., Feeney, K. A. et al. (2012). Peroxiredoxins are conserved markers of circadian rhythms. *Nature* **485**, 459-464.

Finelli, A., Kelkar, A., Song, H.-J., Yang, H. and Konsolaki, M. (2004). A model for studying Alzheimer's Abeta42-induced toxicity in Drosophila melanogaster. *Mol. Cell. Neurosci.* **26**, 365-375.

Fossgreen, A., Brückner, B., Czech, C., Masters, C. L., Beyreuther, K. and Paro, R. (1998). Transgenic Drosophila expressing human amyloid precursor protein show γ-secretase activity and a blistered-wing phenotype. *Proc. Natl. Acad. Sci. USA* **95**, 13703-13708.

Gorman, M. R. and Yellon, S. (2010). Lifespan daily locomotor activity rhythms in a mouse model of amyloid-induced neuropathology. *Chronobiol. Int.* **27**, 1159-1177.

Harrisingh, M. C., Wu, Y., Lnenicka, G. A. and Nitabach, M. N. (2007). Intracellular Ca2+ regulates free-running circadian clock oscillation in vivo. *J. Neurosci.* **27**, 12489-12499.

Hastings, M. H. and Herzog, E. D. (2004). Clock genes, oscillators, and cellular networks in the suprachiasmatic nuclei. *J. Biol. Rhythms* **19**, 400-413.

Helfrich-Förster, C., Shafer, O. T., Wülbeck, C., Grieshaber, E., Rieger, D. and Taghert, P. (2007). Development and morphology of the clock-gene-expressing lateral neurons of Drosophila melanogaster. *J. Comp. Neurol.* **500**, 47-70.

Hermann, C., Yoshii, T., Dusik, V. and Helfrich-Förster, C. (2012). Neuropeptide F immunoreactive clock neurons modify evening locomotor activity and free-running period in Drosophila melanogaster. *J. Comp. Neurol.* **520**, 970-987.

Hodge, J. J. and Stanewsky, R. (2008). Function of the Shaw potassium channel within the Drosophila circadian clock. *PLoS ONE* **3**, e2274.

Huang, J.-K., Ma, P.-L., Ji, S.-Y., Zhao, X.-L., Tan, J.-X., Sun, X.-J. and Huang, F.-D. (2013). Age-dependent alterations in the presynaptic active zone in a Drosophila model of Alzheimer's disease. *Neurobiol. Dis.* **51**, 161-167.

Iijima, K., Liu, H. P., Chiang, A. S., Hearn, S. A., Konsolaki, M. and Zhong, Y. (2004). Dissecting the pathological effects of human Abeta40 and Abeta42 in Drosophila: a potential model for Alzheimer's disease. *Proc. Natl. Acad. Sci. USA* **101**, 6623-6628.

Iijima-Ando, K. and Iijima, K. (2010). Transgenic Drosophila models of Alzheimer's disease and tauopathies. *Brain Struct. Funct.* **214**, 245-262.

Jahn, T. R., Kohlhoff, K. J., Scott, M., Tartaglia, G. G., Lomas, D. A., Dobson, C. M., Vendruscolo, M. and Crowther, D. C. (2011). Detection of early locomotor abnormalities in a Drosophila model of Alzheimer's disease. *J. Neurosci. Methods* **197**, 186-189.

Jo, J., Whitcomb, D. J., Olsen, K. M., Kerrigan, T. L., Lo, S.-C., Bru-Mercier, G., Dickinson, B., Scullion, S., Sheng, M., Collingridge, G. et al. (2011). Aβ(1-42) inhibition of LTP is mediated by a signaling pathway involving caspase-3, Akt1 and GSK-3β. *Nat. Neurosci.* **14**, 545-547.

Jonsson, T., Atwal, J. K., Steinberg, S., Snaedal, J., Jonsson, P. V., Bjornsson, S., Stefansson, H., Sulem, P., Gudbjartsson, D., Maloney, J. et al. (2012). A mutation in APP protects against Alzheimer's disease and age-related cognitive decline. *Nature* **488**, 96-99.

Kaneko, M. and Hall, J. C. (2000). Neuroanatomy of cells expressing clock genes in Drosophila: transgenic manipulation of the period and timeless genes to mark the perikarya of circadian pacemaker neurons and their projections. *J. Comp. Neurol.* **422**, 66-94.

Kaneko, M., Park, J. H., Cheng, Y., Hardin, P. E. and Hall, J. C. (2000). Disruption of synaptic transmission or clock-gene-product oscillations in circadian pacemaker cells of Drosophila cause abnormal behavioral rhythms. *J. Neurobiol.* **43**, 207-233.

Konopka, R. J., Pittendrigh, C. and Orr, D. (1989). Reciprocal behaviour associated with altered homeostasis and photosensitivity of Drosophila clock mutants. *J. Neurogenet.* **6**, 1-10.

Krishnan, N., Rakshit, K., Chow, E. S., Wentzell, J. S., Kretzschmar, D. and Giebultowicz, J. M. (2012). Loss of circadian clock accelerates aging in neurodegeneration-prone mutants. *Neurobiol. Dis.* **45**, 1129-1135.

LaFerla, F. M., Green, K. N. and Oddo, S. (2007). Intracellular amyloid-β in Alzheimer's disease. *Nat. Rev. Neurosci.* **8**, 499-509.

Lesné, S., Koh, M. T., Kotilinek, L., Kayed, R., Glabe, C. G., Yang, A., Gallagher, M. and Ashe, K. H. (2006). A specific amyloid-β protein assembly in the brain impairs memory. *Nature* **440**, 352-357.

Levine, J. D., Funes, P., Dowse, H. B. and Hall, J. C. (2002). Signal analysis of behavioral and molecular cycles. *BMC Neurosci.* **3**, 1.

Lim, C., Chung, B. Y., Pitman, J. L., McGill, J. J., Pradhan, S., Lee, J., Keegan, K. P., Choe, J. and Allada, R. (2007). Clockwork orange encodes a transcriptional repressor important for circadian-clock amplitude in Drosophila. *Curr. Biol.* **17**, 1082-1089.

Locke, J. C., Southern, M. M., Kozma-Bognar, L., Hibberd, V., Brown, P. E., Turner, M. S. and Millar, A. J. (2005). Extension of a genetic network model by iterative experimentation and mathematical analysis. *Mol. Syst. Biol.* **1**, 2005 0013.

Luheshi, L. M., Tartaglia, G. G., Brorsson, A.-C., Pawar, A. P., Watson, I. E., Chiti, F., Vendruscolo, M., Lomas, D. A., Dobson, C. M. and Crowther, D. C. (2007). Systematic in vivo analysis of the intrinsic determinants of amyloid β pathogenicity. *PLoS Biol.* **5**, e290.

Luo, W., Chen, W. F., Yue, Z., Chen, D., Sowcik, M., Sehgal, A. and Zheng, X. (2012). Old flies have a robust central oscillator but weaker behavioral rhythms that can be improved by genetic and environmental manipulations. *Aging Cell* **11**, 428-438.

Markesbery, W. R., Kryscio, R. J., Lovell, M. A. and Morrow, J. D. (2005). Lipid peroxidation is an early event in the brain in amnestic mild cognitive impairment. *Ann. Neurol.* **58**, 730-735.

Marrus, S. B., Zeng, H. and Rosbash, M. (1996). Effect of constant light and circadian entrainment of perS flies: evidence for light-mediated delay of the negative feedback loop in Drosophila. *EMBO J.* **15**, 6877-6886.

Maywood, E. S., Reddy, A. B., Wong, G. K., O'Neill, J. S., O'Brien, J. A., McMahon, D. G., Harmar, A. J., Okamura, H. and Hastings, M. H. (2006). Synchronization and maintenance of timekeeping in suprachiasmatic circadian clock cells by neuropeptidergic signaling. *Curr. Biol.* **16**, 599-605.

Mohawk, J. A., Green, C. B. and Takahashi, J. S. (2012). Central and peripheral circadian clocks in mammals. *Annu. Rev. Neurosci.* **35**, 445-462.

Nakamura, T. J., Nakamura, W., Yamazaki, S., Kudo, T., Cutler, T., Colwell, C. S. and Block, G. D. (2011). Age-related decline in circadian output. *J. Neurosci.* **31**, 10201-10205.

Ng, F. S., Tangredi, M. M. and Jackson, F. R. (2011). Glial cells physiologically modulate clock neurons and circadian behavior in a calcium-dependent manner. *Curr. Biol.* **21**, 625-634.

Nilsberth, C., Westlind-Danielsson, A., Eckman, C. B., Condron, M. M., Axelman, K., Forsell, C., Stenh, C., Luthman, J., Teplow, D. B., Younkin, S. G. et al. (2001). The 'Arctic' APP mutation (E693G) causes Alzheimer's disease by enhanced Abeta protofibril formation. *Nat. Neurosci.* **4**, 887-893.

Nitabach, M. N., Blau, J. and Holmes, T. C. (2002). Electrical silencing of Drosophila pacemaker neurons stops the free-running circadian clock. *Cell* **109**, 485-495.
Nunomura, A., Perry, G., Aliev, G., Hirai, K., Takeda, A., Balraj, E. K., Jones, P. K., Ghanbari, H., Wataya, T., Shimohama, S. et al. (2001). Oxidative damage is the earliest event in Alzheimer disease. *J. Neuropathol. Exp. Neurol.* **60**, 759-767.
O'Neill, J. S., van Ooijen, G., Dixon, L. E., Troein, C., Corellou, F., Bouget, F.-Y., Reddy, A. B. and Millar, A. J. (2011). Circadian rhythms persist without transcription in a eukaryote. *Nature* **469**, 554-558.
Ono, K., Condron, M. M. and Teplow, D. B. (2009). Structure-neurotoxicity relationships of amyloid β-protein oligomers. *Proc. Natl. Acad. Sci. USA* **106**, 14745-14750.
Pallier, P. N., Maywood, E. S., Zheng, Z., Chesham, J. E., Inyushkin, A. N., Dyball, R., Hastings, M. H. and Morton, A. J. (2007). Pharmacological imposition of sleep slows cognitive decline and reverses dysregulation of circadian gene expression in a transgenic mouse model of Huntington's disease. *J. Neurosci.* **27**, 7869-7878.
Park, N., Cheon, S., Son, G. H., Cho, S. and Kim, K. (2012). Chronic circadian disturbance by a shortened light-dark cycle increases mortality. *Neurobiol. Aging* **33**, 1122.e1111-1122.e1122.
Paudel, M. L., Taylor, B. C., Ancoli-Israel, S., Blackwell, T., Stone, K. L., Tranah, G., Redline, S., Cummings, S. R., Ensrud, K. E.; Osteoporotic Fractures in Men (MrOS) Study (2010). Rest/activity rhythms and mortality rates in older men: MrOS Sleep Study. *Chronobiol. Int.* **27**, 363-377.
Peng, Y., Stoleru, D., Levine, J. D., Hall, J. C. and Rosbash, M. (2003). Drosophila free-running rhythms require intercellular communication. *PLoS Biol.* **1**, e13.
Philipson, O., Lord, A., Gumucio, A., O'Callaghan, P., Lannfelt, L. and Nilsson, L. N. (2010). Animal models of amyloid-β-related pathologies in Alzheimer's disease. *FEBS J.* **277**, 1389-1409.
Pittendrigh, C. S. and Minis, D. H. (1972). Circadian systems: longevity as a function of circadian resonance in Drosophila melanogaster. *Proc. Natl. Acad. Sci. USA* **69**, 1537-1539.
Prinz, P. N., Vitaliano, P. P., Vitiello, M. V., Bokan, J., Raskind, M., Peskind, E. and Gerber, C. (1982). Sleep, EEG and mental function changes in senile dementia of the Alzheimer's type. *Neurobiol. Aging* **3**, 361-370.
Rakshit, K., Krishnan, N., Guzik, E. M., Pyza, E. and Giebultowicz, J. M. (2012). Effects of aging on the molecular circadian oscillations in Drosophila. *Chronobiol. Int.* **29**, 5-14.
Renn, S. C., Park, J. H., Rosbash, M., Hall, J. C. and Taghert, P. H. (1999). A pdf neuropeptide gene mutation and ablation of PDF neurons each cause severe abnormalities of behavioral circadian rhythms in *Drosophila*. *Cell* **99**, 791-802.
Rezával, C., Berni, J., Gorostiza, E. A., Werbajh, S., Fagilde, M. M., Fernández, M. P., Beckwith, E. J., Aranovich, E. J., Sabio y García, C. A. and Ceriani, M. F. (2008). A functional misexpression screen uncovers a role for enabled in progressive neurodegeneration. *PLoS ONE* **3**, e3332.
Rival, T., Page, R. M., Chandraratna, D. S., Sendall, T. J., Ryder, E., Liu, B., Lewis, H., Rosahl, T., Hider, R., Camargo, L. M. et al. (2009). Fenton chemistry and oxidative stress mediate the toxicity of the β-amyloid peptide in a Drosophila model of Alzheimer's disease. *Eur. J. Neurosci.* **29**, 1335-1347.
Sehadova, H., Glaser, F. T., Gentile, C., Simoni, A., Giesecke, A., Albert, J. T. and Stanewsky, R. (2009). Temperature entrainment of Drosophila's circadian clock involves the gene nocte and signaling from peripheral sensory tissues to the brain. *Neuron* **64**, 251-266.
Sekine, T., Yamaguchi, T., Hamano, K., Siomi, H., Saez, L., Ishida, N. and Shimoda, M. (2008). Circadian phenotypes of Drosophila fragile x mutants in alternative genetic backgrounds. *Zoolog. Sci.* **25**, 561-571.
Shankar, G. M., Li, S., Mehta, T. H., Garcia-Munoz, A., Shepardson, N. E., Smith, I., Brett, F. M., Farrell, M. A., Rowan, M. J., Lemere, C. A. et al. (2008). Amyloid-β protein dimers isolated directly from Alzheimer's brains impair synaptic plasticity and memory. *Nat. Med.* **14**, 837-842.
Speretta, E., Jahn, T. R., Tartaglia, G. G., Favrin, G., Barros, T. P., Imarisio, S., Lomas, D. A., Luheshi, L. M., Crowther, D. C. and Dobson, C. M. (2012). Expression in Drosophila of tandem amyloid β peptides provides insights into links between aggregation and neurotoxicity. *J. Biol. Chem.* **287**, 20748-20754.
Stanewsky, R., Jamison, C. F., Plautz, J. D., Kay, S. A. and Hall, J. C. (1997). Multiple circadian-regulated elements contribute to cycling period gene expression in Drosophila. *EMBO J.* **16**, 5006-5018.
Sterniczuk, R., Dyck, R. H., Laferla, F. M. and Antle, M. C. (2010). Characterization of the 3xTg-AD mouse model of Alzheimer's disease: part 1. Circadian changes. *Brain Res.* **1348**, 139-148.
Stoleru, D., Peng, Y., Agosto, J. and Rosbash, M. (2004). Coupled oscillators control morning and evening locomotor behaviour of Drosophila. *Nature* **431**, 862-868.
Stoleru, D., Peng, Y., Nawathean, P. and Rosbash, M. (2005). A resetting signal between Drosophila pacemakers synchronizes morning and evening activity. *Nature* **438**, 238-242.
Swaab, D. F., Fliers, E. and Partiman, T. S. (1985). The suprachiasmatic nucleus of the human brain in relation to sex, age and senile dementia. *Brain Res.* **342**, 37-44.
Swaab, D. F., Fisser, B., Kamphorst, W. and Troost, D. (1988). The human suprachiasmatic nucleus; neuropeptide changes in senium and Alzheimer's disease. *Basic Appl. Histochem.* **32**, 43-54.
Tang, Y., Scott, D. A., Das, U., Edland, S. D., Radomski, K., Koo, E. H. and Roy, S. (2012). Early and selective impairments in axonal transport kinetics of synaptic cargoes induced by soluble amyloid β-protein oligomers. *Traffic* **13**, 681-693.
Tate, B., Aboody-Guterman, K. S., Morris, A. M., Walcott, E. C., Majocha, R. E. and Marotta, C. A. (1992). Disruption of circadian regulation by brain grafts that overexpress Alzheimer beta/A4 amyloid. *Proc. Natl. Acad. Sci. USA* **89**, 7090-7094.
Tomic, J. L., Pensalfini, A., Head, E. and Glabe, C. G. (2009). Soluble fibrillar oligomer levels are elevated in Alzheimer's disease brain and correlate with cognitive dysfunction. *Neurobiol. Dis.* **35**, 352-358.
Tranah, G. J., Blackwell, T., Stone, K. L., Ancoli-Israel, S., Paudel, M. L., Ensrud, K. E., Cauley, J. A., Redline, S., Hillier, T. A., Cummings, S. R. et al.; SOF Research Group (2011). Circadian activity rhythms and risk of incident dementia and mild cognitive impairment in older women. *Ann. Neurol.* **70**, 722-732.
Umezaki, Y., Yoshii, T., Kawaguchi, T., Helfrich-Förster, C. and Tomioka, K. (2012). Pigment-dispersing factor is involved in age-dependent rhythm changes in Drosophila melanogaster. *J. Biol. Rhythms* **27**, 423-432.
Veleri, S., Brandes, C., Helfrich-Förster, C., Hall, J. C. and Stanewsky, R. (2003). A self-sustaining, light-entrainable circadian oscillator in the Drosophila brain. *Curr. Biol.* **13**, 1758-1767.
Volicer, L., Harper, D. G., Manning, B. C., Goldstein, R. and Satlin, A. (2001). Sundowning and circadian rhythms in Alzheimer's disease. *Am. J. Psychiatry* **158**, 704-711.
Whalen, B. M., Selkoe, D. J. and Hartley, D. M. (2005). Small non-fibrillar assemblies of amyloid β-protein bearing the Arctic mutation induce rapid neuritic degeneration. *Neurobiol. Dis.* **20**, 254-266.
Wisor, J. P., Edgar, D. M., Yesavage, J., Ryan, H. S., McCormick, C. M., Lapustea, N. and Murphy, G. M., Jr (2005). Sleep and circadian abnormalities in a transgenic mouse model of Alzheimer's disease: a role for cholinergic transmission. *Neuroscience* **131**, 375-385.
Wu, Y.-H. and Swaab, D. F. (2007). Disturbance and strategies for reactivation of the circadian rhythm system in aging and Alzheimer's disease. *Sleep Med.* **8**, 623-636.
Wu, Y.-H., Fischer, D. F., Kalsbeek, A., Garidou-Boof, M.-L., van der Vliet, J., van Heijningen, C., Liu, R.-Y., Zhou, J.-N. and Swaab, D. F. (2006). Pineal clock gene oscillation is disturbed in Alzheimer's disease, due to functional disconnection from the "master clock". *FASEB J.* **20**, 1874-1876.

Figure S1

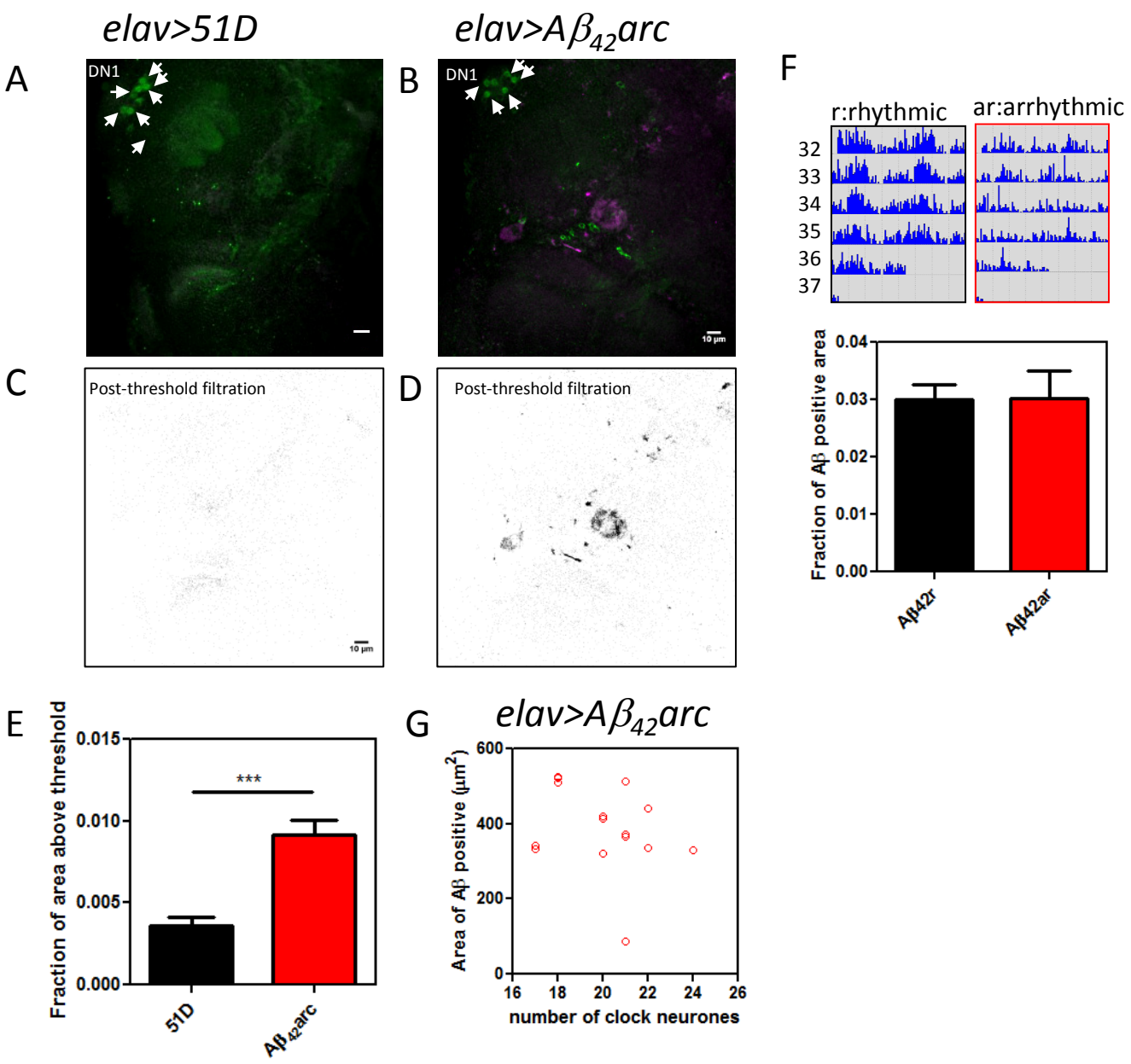
elav>51D
elav>Aβ42arc
A
DN1
B
DN1
C
Post-threshold filtration
D
Post-threshold filtration
F
r:rhythmic
ar:arrhythmic
32
33
34
35
36
37
Fraction of Aβ positive area
0.04
0.03
0.02
0.01
0.00
Aβ42r
Aβ42ar
E
Fraction of area above threshold
0.015
0.010
0.005
0.000
***
51D
Aβ42arc
G
elav>Aβ42arc
Area of Aβ positive (μm2)
600
400
200
0
16
18
20
22
24
26
number of clock neurones

Figure S2

A

elav>51D, DN1s

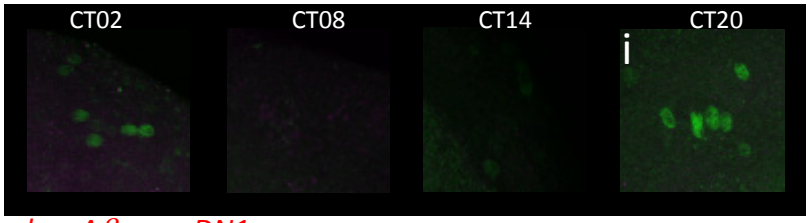

elav>Aβ42arc, DN1s

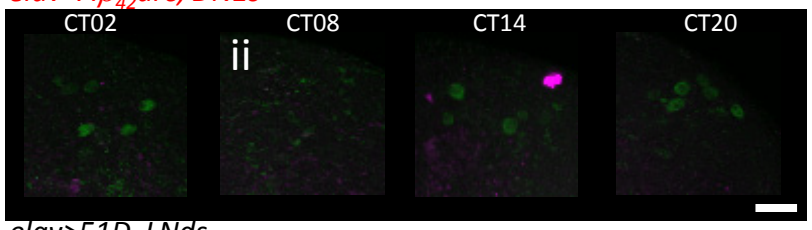

elav>51D, LNds

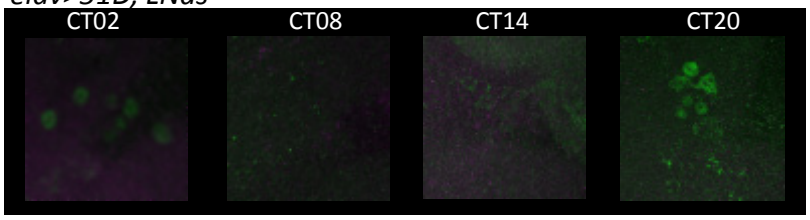

elav>Aβ42arc, LNds

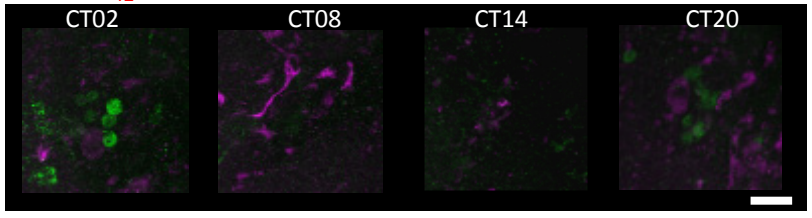

elav>51D, sLNvs

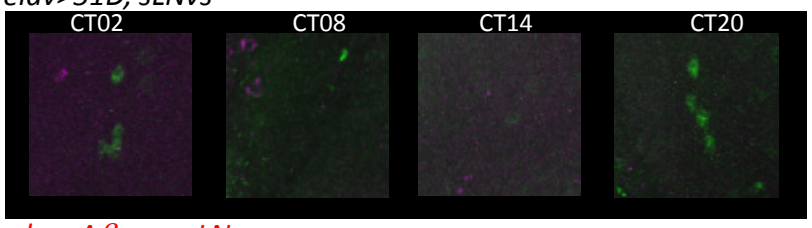

elav>Aβ42arc sLNvs

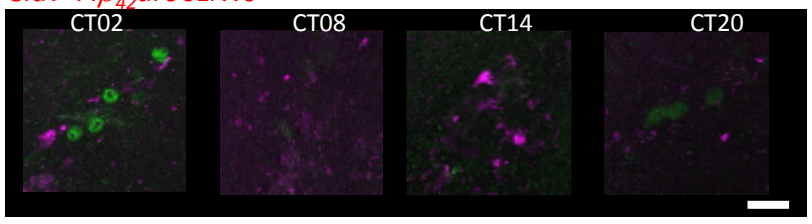

B

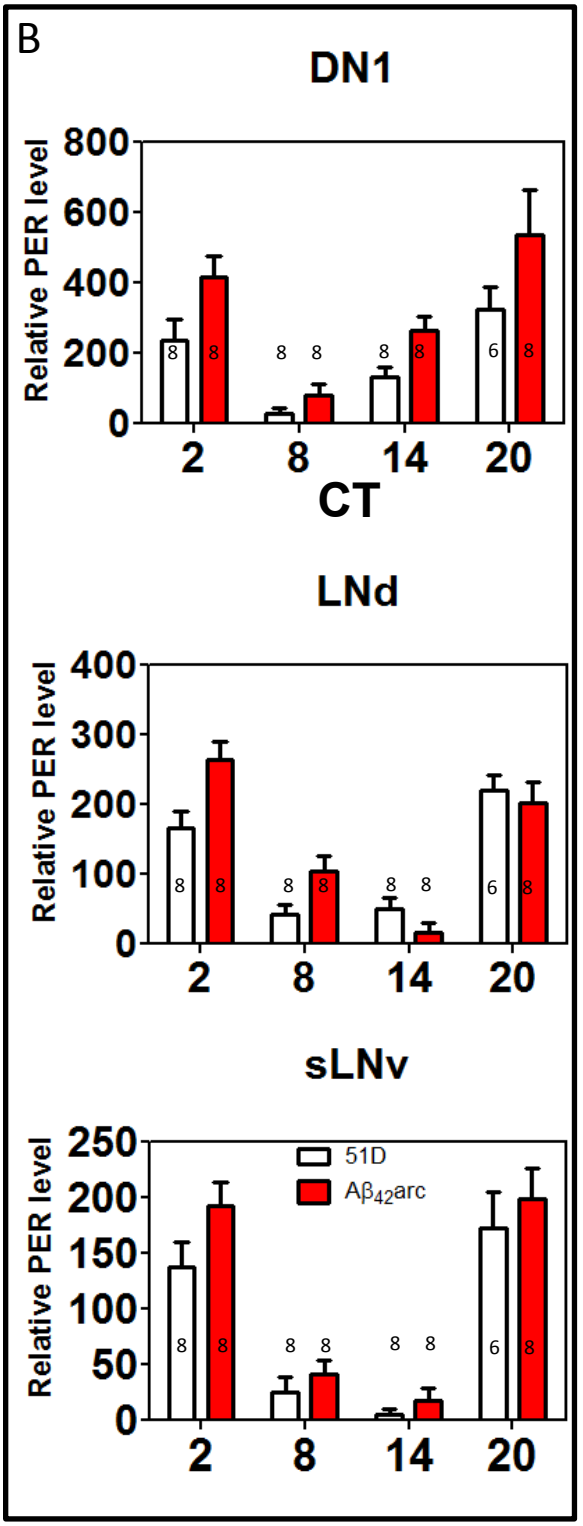

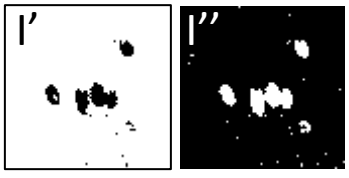

Mi'= mean intensity in the black area (Area.i')
Mi''= mean intensity in the black area (Area.i'')
Relative Period level= Area.i' x (Mi'-Mi'')/ Mi''

Figure S3

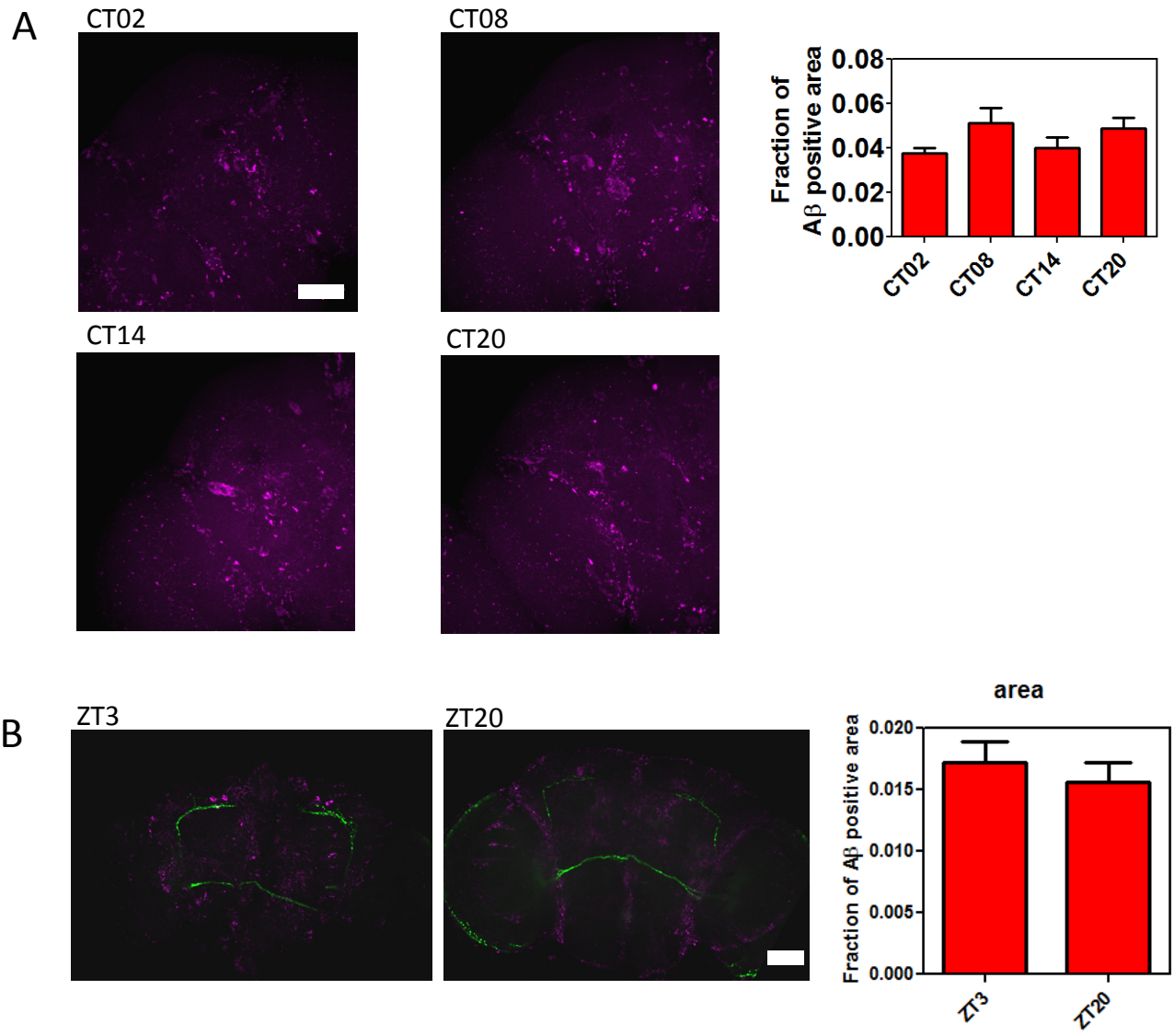
A
CT02
CT08
CT14
CT20
Fraction of Aβ positive area
0.08
0.06
0.04
0.02
0.00
CT02
CT08
CT14
CT20
B
ZT3
ZT20
area
Fraction of Aβ positive area
0.020
0.015
0.010
0.005
0.000
ZT3
ZT20

Figure S4

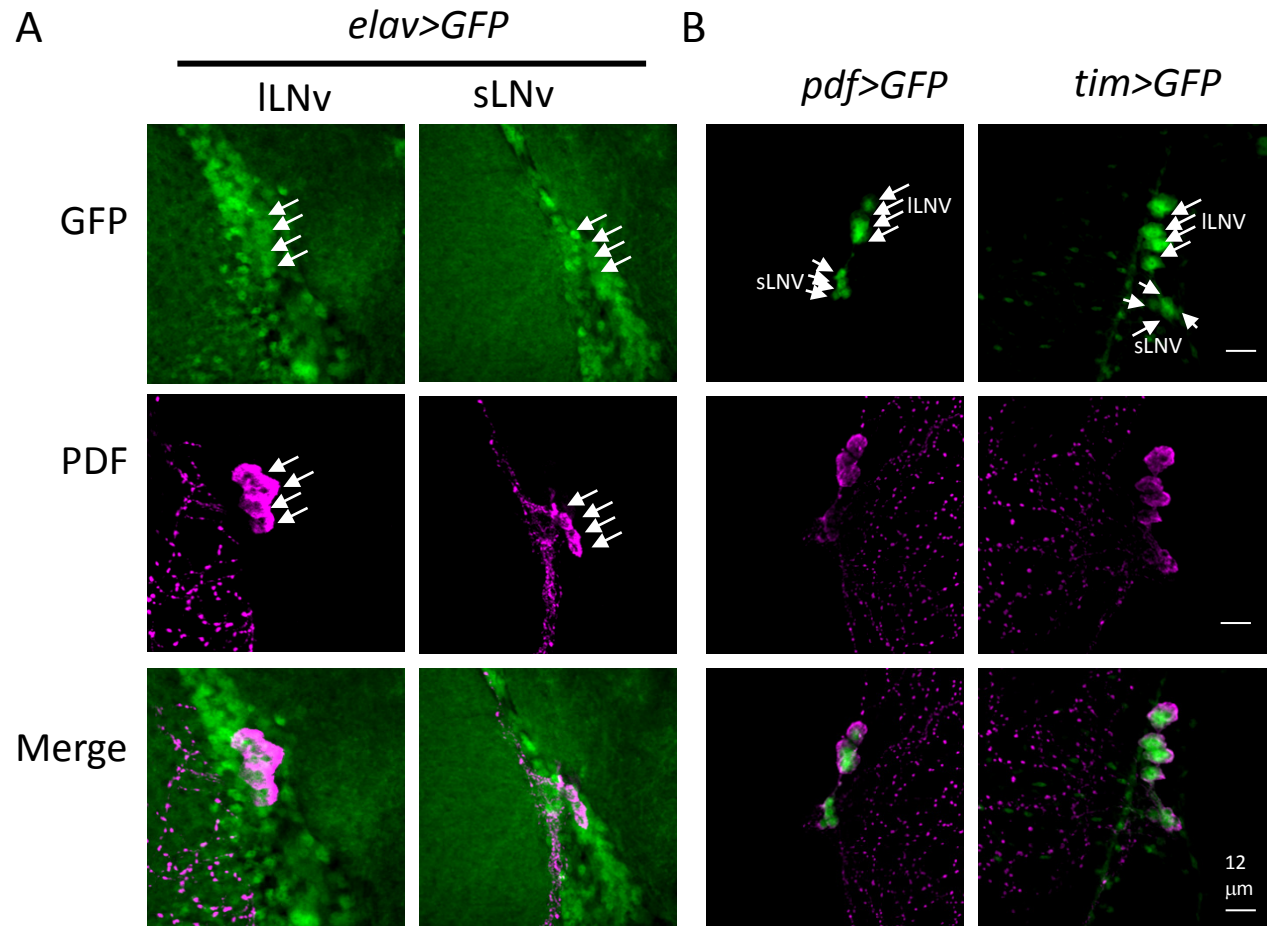
A
elav>GFP
lLNv
sLNv
GFP
PDF
Merge
B
pdf>GFP
tim>GFP
lLNV
sLNV
lLNV
sLNV
12 µm

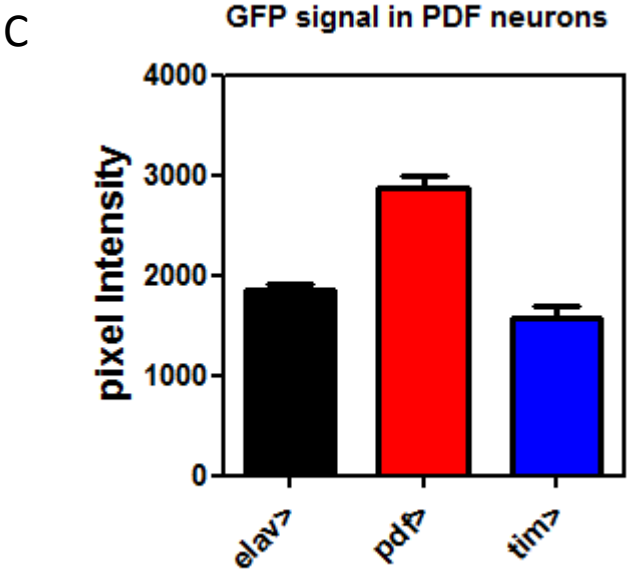
C
GFP signal in PDF neurons
pixel Intensity
4000
3000
2000
1000
0
elav>
pdf>
tim>

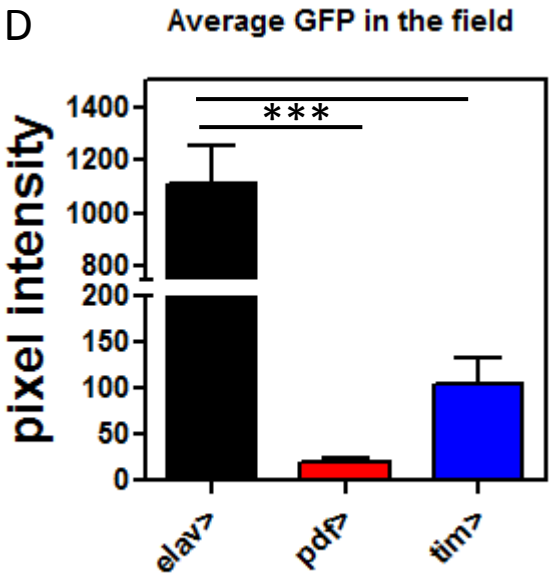
D
Average GFP in the field
pixel intensity
***
1400
1200
1000
800
200
150
100
50
0
elav>
pdf>
tim>

Figure S5

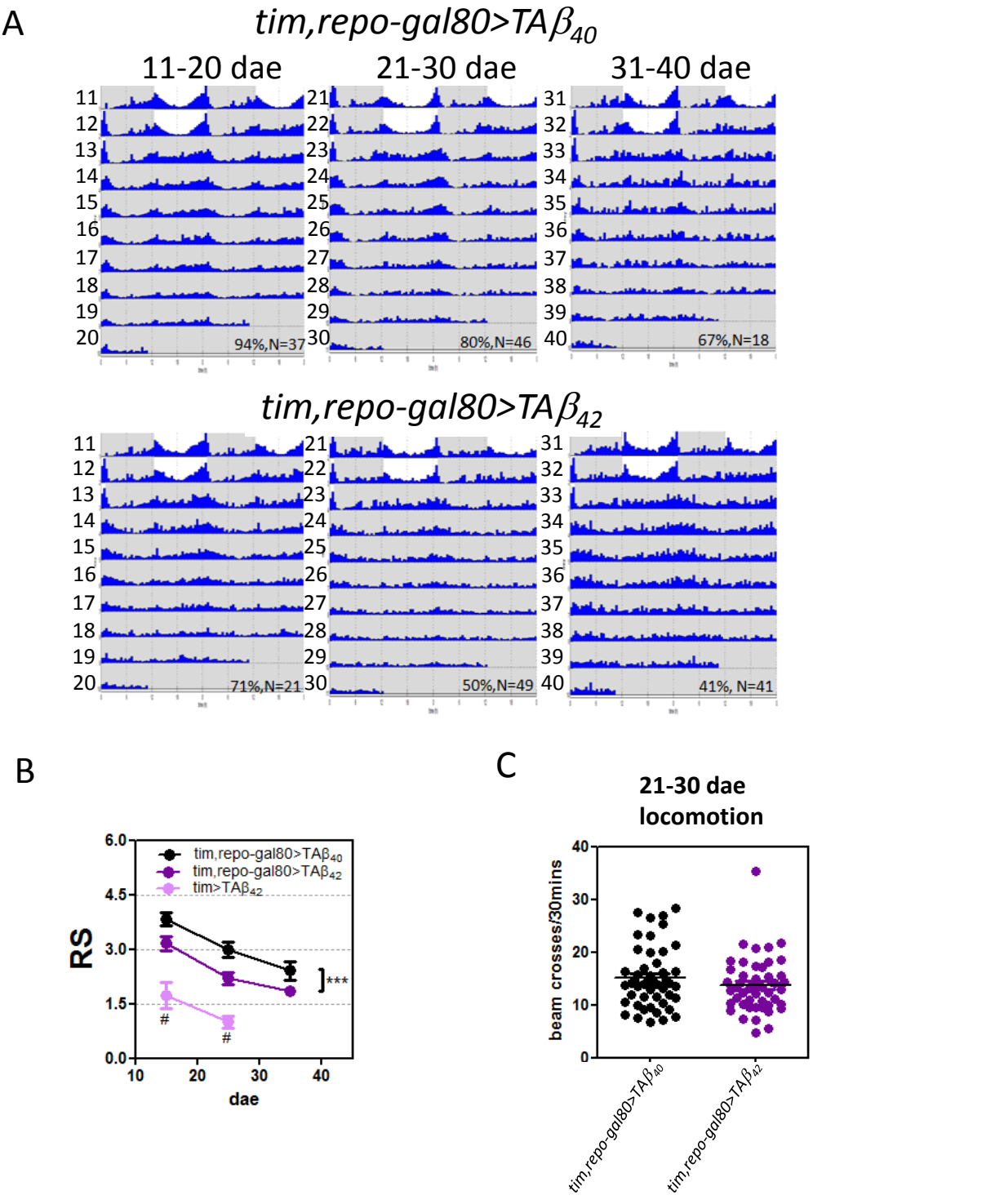
A
tim,repo-gal80>TAβ40
11-20 dae
21-30 dae
31-40 dae
94%,N=37
80%,N=46
67%,N=18
tim,repo-gal80>TAβ42
71%,N=21
50%,N=49
41%, N=41
B
tim,repo-gal80>TAβ40
tim,repo-gal80>TAβ42
tim>TAβ42
RS
dae
***
#
#
C
21-30 dae
locomotion
beam crosses/30mins
tim,repo-gal80>TAβ40
tim,repo-gal80>TAβ42

Figure S6

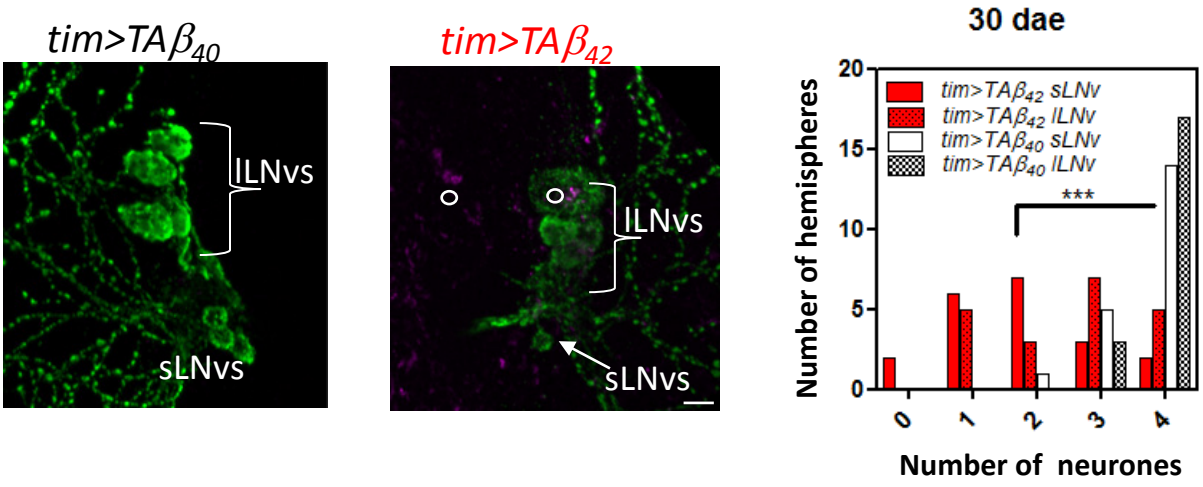
tim>TAβ40
lLNvs
sLNvs
tim>TAβ42
lLNvs
sLNvs
30 dae
tim>TAβ42 sLNv
tim>TAβ42 lLNv
tim>TAβ40 sLNv
tim>TAβ40 lLNv
***
Number of hemispheres
Number of neurones
0
5
10
15
20
0
1
2
3
4

Figure S1. Aβ plaque density in the fly brains does not correlate with the number of clock neurones or with rhythmicity. Representative images of *elav>51D* control (A) and *elav>Aβ$_{42}$arc* brains (B) show areas that were immunoreactive for Period (green, arrows, DN1s shown only) and Aβ (magenta). A threshold signal intensity in the magenta channel was chosen so that the Aβ positive signal (C, *elav>51D* & D, *elav>Aβ$_{42}$arc*) faithfully represents the appearance of the raw image. The area above threshold (μm^2) was divided by the total area in the field to calculate "fraction of Aβ positive area". A significantly higher fraction of the area is Aβ-positive in Aβ$_{42}$arc-expressing fly brains as compared to controls (E, mean±SEM, p<0.001 *Student* t-test, the same data set from Figure 3C and D). After five days of circadian behaviour testing, rhythmically robust (Aβ$_{42}$r, RS>1.5, n=3) and arrhythmic (Aβ$_{42}$ar, RS≤1.5, n=6) 37 dae old *elav>Aβ$_{42}$* flies were re-grouped in separate food vials. Following a further 3 days in LD the brains were dissected at ZT3 (F). Areas of positive Aβ signal (mean±SEM) were quantified and no difference was found between the two groups (*Student t-test*). Furthermore, no correlation (p=0.37) exists between the number of Period positive clock neurones and the density of Aβ plaques (area of Aβ positive) for *elav>Aβ$_{42}$arc* (G, 30 dae, ZT22, the same dataset as in Figure 3). Scale bars: 10μm. ZT denotes zeitgeber time with ZT0 indicating dawn and ZT12 dusk during LD cycles.

Figure S2. Robust Period oscillation in clock neurones in behaviourally arrhythmic Aβ$_{42}$arc-expressing fly brains during constant darkness. Period (green ovals) and Aβ (magenta) staining was performed for 28 dae old controls (*elav>51D*) and *elav>Aβ$_{42}$arc* flies that have been reared in constant darkness. The fly brains were sampled at the four indicated time points in the second day of constant darkness (CT02, CT08, CT14 and CT20); CT denotes constant time, with CT00 indicating subjective dawn and CT12 subjective dusk. (A) Period and Aβ signals in the indicated clock neurones for *elav>Aβ$_{42}$arc* flies and controls at the four time points. The average Period signal in each image was quantified (e.g. panel i, i' and i'') by measuring the mean pixel intensity (Mi') in the area within clock neurones in the green channel (i'). Similarly the background pixel intensities (Mi'') in the area adjacent to clock neurones (i'') were also quantified. **Relative Period level** was then calculated by subtracting and normalising the background (Mi'-Mi''/Mi'') and multiplying with the area containing clock neurones (Area.i') to account for the signal variation in the background and the number of detectable clock neurones at each images (modified from Chen et al., 2011). For time points in which Period staining cannot be identified (e.g. ii), the relative Period level was assigned as zero. (B) Both control (white bars)

and $A\beta_{42}$arc expressing flies (red bars) showed clear oscillation of Period levels (mean±SEM) across the four time points (non-parametric one-way ANOVA, $p<0.001$). The numbers of brain hemispheres observed at each time point and genotypes are indicated by the respective bar. Scale bars: 10μm.

Figure S3. Aβ plaque density does not show circadian oscillation. (A) Aβ staining (magenta) was quantified for the $A\beta_{42}$arc-expressing brain hemispheres shown in Figure S2. No differences in the fraction of Aβ positive area (mean±SEM) were observed at the four indicated time points during constant darkness. (B) There was no difference in the fraction of Aβ positive area (magenta, mean±SEM) between ZT3 and ZT20 during LD cycles in the image stacks of *tim,repo-gal80>TAβ_{42}* fly brains (from Figure 6C). Green: PDF staining. Scale bars: 50μm

Figure S4. Comparing GFP expression in PDF neurones using elav-, pdf- and tim-gal4 driver constructs. Representative images show that UAS-driven GFP intensity (green) was similar for each of the three gal4 drivers used in this study. Quantification was performed by measuring GFP signal within cells expressing endogenous PDF peptide (magenta, arrows, lLNvs and sLNvs) in *elav>GFP* (n=125 neurones, A) and *pdf>GFP* (n=56, B) and *tim>GFP* (n=44, B) male fly brains. Confocal image stacks along frontal-posterior axis were taken to include all PDF neurones. The GFP signal within the cellular outline of individual PDF neurons was measured by ImageJ system (pixel intensity in greyscale, maximum=4096, C). The average GFP signal in a fixed field of 318 μm^2 was calculated for all the stacked images for each genotype (D). The number of fields used to determine the average background GFP staining was 5 for *elav>GFP*, 4 for *pdf>GFP* and 6 for *tim>GFP*. Asterisks mark significant difference as determined by non-parametric one-way ANOVA (***=$p<0.001$).

Figure S5. Restricting TAβ_{42} expression to clock neurones resulted in intermediate circadian arrhythmicity. (A) Representative actograms are shown for *tim,repo-gal80>TAβ_{42}* (reduced rhythmicity) and control *tim,repo-gal80>TAβ_{40}* at the indicated ages. Total number of flies tested (n) and percentage of rhythmic flies in each genotype (%) are indicated. (B) RS values for *tim,repo-gal80>TAβ_{42}* and *tim,repo-gal80>TAβ_{40}* flies at all tested age groups are plotted. The significance of overall differences in the RS values between the two genotypes was determined by two-way ANOVA (***: $p<0.001$). Significant differences in the RS values was identified by one-way ANOVA (#: $p<0.05$) among the four groups of flies *tim,repo-gal80>TAβ_{42}* (11-20 dae and 21-30 dae) and *tim>TAβ_{42}* flies (n=8, 11-20 dae and n=9, 21-30 dae).

The tim(67) gal4 driver line was used in this experiment. (C) No difference in average locomotor activity (i.e., beam crosses) were found between *tim,repo-gal80>TAβ_{42}* and *tim,repo-gal80>TAβ_{40}* flies aged 21-30 dae (re-analysis from A).

Figure S6. TAβ_{42} expression in clock cells resulted in loss of PDF neurones. Drastic loss of PDF neurons (green) coincided with Aβ positive staining (magenta, circles, both inside and outside of PDF neurones) was found in *tim>TAβ_{42}* fly brain (n=20, in brain hemisphere) as compared to *tim>TAβ_{40}* flies (n=20). The number of PDF neurones was counted for both sLNvs and lLNvs in the two genotypes. Significant difference determined by χ_2-test was found between the two genotypes for both sLNvs and lLNvs (***: p<0.001, see Materials and Methods).

Table S1. Summary of rhythmic luciferase signal from *8.0-luc* flies

age	genotype	R	Sum	R%	Amp
13-17 dae	*elav>51D*	4	12	33%	3.0±0.5
13-17 dae	*elav> Aβ42arc*	11	12	92%	4.5±0.2
16-20 dae	*elav>51D*	4	12	33%	3.2±0.5
16-20 dae	*elav> Aβ42arc*	3	12	25%	3.2±0.2
19-23 dae	*elav>51D*	3	12	25%	2.1±0.2
19-23 dae	*elav> Aβ42arc*	5	12	42%	3.8±0.3
20-24 dae	*elav>51D*	4	12	33%	3.0±0.4
20-24 dae	*elav> Aβ42arc*	4	12	33%	2.6±0.3
23-27 dae	*elav>51D*	3	12	25%	3.5±0.7
23-27 dae	*elav> Aβ42arc*	5	12	42%	3.1±0.3
25-29 dae	*elav>51D*	3	12	25%	2.4±0.3
25-29 dae	*elav> Aβ42arc*	6	12	50%	2.8±0.5
19-23 dae	*tim>TAβ40*	23	28	82%	3.8±0.3
19-23 dae	*tim>TAβ42*	22	26	85%	*2.7±0.2
25-29 dae	*tim>TAβ40*	15	19	79%	2.9±0.1
25-29 dae	*tim>TAβ42*	12	16	75%	2.6±0.7
27-31 dae	*tim>TAβ40*	10	16	63%	3.1±0.5
27-31 dae	*tim>TAβ42*	6	16	38%	3.7±0.4

R: number of flies containing rhythmic luciferase signal (rel-amp error <0.7), Sum: number of fly tested. Amp (mean±SEM): relative amplitude for rhythmic luciferase. Kruskal-Wallis ANOVA statistics with Dunn's Multiple Comparison test are used to determine significant difference in amplitude as compared to age matched controls (*:$p<0.01$). No difference are found in all pair-wise comparison between *elav>51D* and *elav>Aβ42arc*. A minor difference in amplitude was detected for 19-23 dae old *tim>TAβ42/8.0-luc*. This difference is unlikely to cause circadian arrhythmicity because the amplitude is similar to the behaviourally rhythmic control at older ages (c.f. *tim>TAβ40* and *tim>TAβ40/8.0-luc*, Table 1 and *tim>TAβ40* flies, 25-29 dae, Table S1).